

See discussions, stats, and author profiles for this publication at: <https://www.researchgate.net/publication/230794562>

# Suppression of $\beta$ -Hydride Chain Transfer in Nickel(II)-Catalyzed Ethylene Polymerization via Weak Fluorocarbon Ligand–Product Interactions

ARTICLE in ORGANOMETALLICS · MAY 2012

Impact Factor: 4.13 · DOI: 10.1021/Om3002735

---

CITATIONS

33

---

READS

22

## 6 AUTHORS, INCLUDING:



Changle Chen

University of Science and Technology of China

57 PUBLICATIONS 617 CITATIONS

[SEE PROFILE](#)



Massimiliano Delferro

Northwestern University

35 PUBLICATIONS 504 CITATIONS

[SEE PROFILE](#)



Alceo Macchioni

Università degli Studi di Perugia

161 PUBLICATIONS 4,916 CITATIONS

[SEE PROFILE](#)

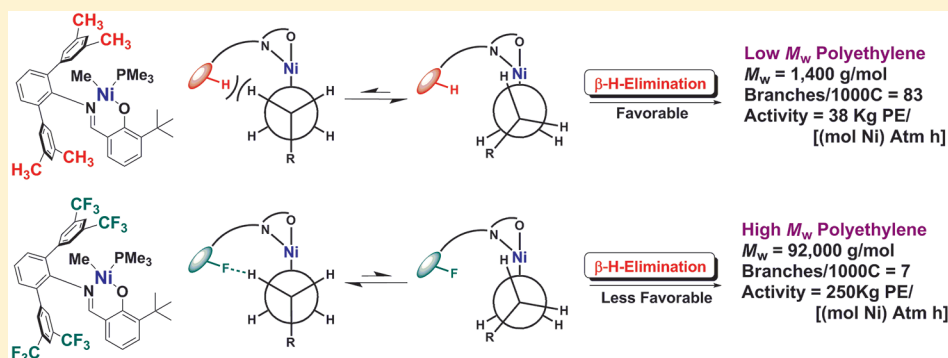
# Suppression of $\beta$ -Hydride Chain Transfer in Nickel(II)-Catalyzed Ethylene Polymerization via Weak Fluorocarbon Ligand–Product Interactions

Michael P. Weberski, Jr.,<sup>†</sup> Changle Chen,<sup>†</sup> Massimiliano Delferro,\*<sup>\*,†</sup> Cristiano Zuccaccia,<sup>‡</sup> Alceo Macchioni,<sup>‡</sup> and Tobin J. Marks<sup>\*,†</sup>

<sup>†</sup>Department of Chemistry, Northwestern University, Evanston, Illinois 60208-3113, United States

<sup>‡</sup>Dipartimento di Chimica, Università degli Studi di Perugia, Via Elce di Sotto, 8-06123 Perugia, Italy

## Supporting Information



**ABSTRACT:** The synthesis and characterization of two neutrally charged Ni(II) ethylene polymerization catalysts, [2-*tert*-butyl-6-((2,6-(3,5-dimethylphenyl)phenylimino)methyl)phenolato]nickel(II) methyl trimethylphosphine ( $(\text{CH}_3)_2\text{FI-Ni}$ ) and [2-*tert*-butyl-6-((2,6-(3,5-bis(trifluoromethyl)phenyl)phenylimino)methyl)phenolato]nickel(II) methyl trimethylphosphine ( $(\text{CF}_3)_2\text{FI-Ni}$ ) are reported. In the presence of a  $\text{Ni}(\text{COD})_2$  cocatalyst, these catalysts produce markedly different polyethylenes: densely branched oligomers with  $M_w = 1.4 \times 10^3 \text{ g mol}^{-1}$  for  $(\text{CH}_3)_2\text{FI-Ni}$  vs lightly branched polyethylenes with  $M_w = 92 \times 10^3 \text{ g mol}^{-1}$  for  $(\text{CF}_3)_2\text{FI-Ni}$  and with  $\sim 6.5\times$  the polymerization activity and with much greater performance thermal stability. HOESY 2D  $^{19}\text{F}$ ,  $^1\text{H}$  NMR spectra of a model Ni-ethyl compound, [2-*tert*-butyl-6-((2,6-(3,5-bis(trifluoromethyl)phenyl)phenylimino)methyl)phenolato]nickel(II) ethyl 2,4-lutidine ( $(\text{CF}_3)_2\text{FI-Ni-Et}$ ), indicate non-negligible  $\text{C}_\beta-\text{H}_\beta\cdots\text{F}_3\text{C}$  through-space dipolar interactions, and molecular modeling reveals that  $\text{C}_\beta-\text{H}_\beta\cdots\text{F}(\text{C})$  distances can be as small as  $\sim 2.61 \text{ \AA}$  during the polymerization process. Furthermore, there is no structural or spectroscopic evidence for fluorocarbon inductive effects on the structure, bonding, and reactivity of these complexes, and a catalyst with  $\text{CF}_3$  introduced  $\beta$  to the imino N produces only low- $M_w$  oligomers with low activity. These results argue that weak (ligand)C–F $\cdots$ H–C(polymer) interactions can significantly influence the chain transfer characteristics of these catalysts.

## INTRODUCTION

Group 10 olefin polymerization catalysis<sup>1,2</sup> has advanced substantially<sup>3</sup> since the pioneering discovery by Brookhart and co-workers<sup>4</sup> of highly active cationic Ni(II) and Pd(II) catalysts supported by bulky aryl-diimine ligands (Chart 1, A). These catalysts effect ethylene polymerization at substantial rates, as well as the copolymerization of ethylene with polar comonomers such as acrylates, vinyl ketones, silyl vinyl ethers, acrylonitrile, and vinyl acetate.<sup>3d,j,o,4d,5</sup> Ni(II) catalysts also produce highly branched polyethylenes through sequences of rapid  $\beta$ -H elimination/reinsertion termed “chain-walking”.<sup>1i,6</sup> Additionally, highly active neutrally charged Ni(II) phenoxyiminato ethylene polymerization catalysts (Chart 1, B), activated with the phosphine scavenger  $\text{Ni}(\text{COD})_2$  or  $\text{B}(\text{C}_6\text{F}_5)_3$ , developed by Grubbs and co-workers,<sup>7</sup> are tolerant to solvent polar functionality and are competent to coenchain polar substituted norbornenes into polyethylene backbones. We

recently demonstrated that (catalytic center) $\cdots$ (catalytic center) cooperative effects in bimetallic Ni(II) phenoxyiminato ethylene polymerization catalysts (Chart 1, C), as well as bimetallic CGC-based group 4 catalysts,<sup>8</sup> significantly enhance polyethylene branching and  $M_w$  as well as polar comonomer enchainment via very different mechanisms.<sup>9</sup> Despite these significant advances, further enhancement of group 10 polymerization catalyst activity, product molecular weight, and resistance to poorly understood deactivation processes would be highly desirable.

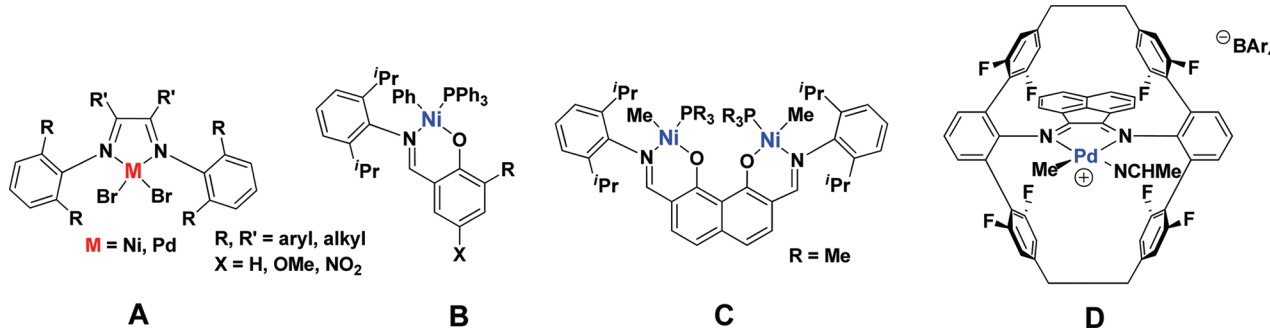
With regard to modifying such catalysts, introducing ligand fluorine substituents in Ni(II) and Pd(II)  $\alpha$ -diimine catalysts D was reported to enhance polyethylene  $M_w$  and catalyst thermal stability, albeit at the cost of lower polymerization activity

Received: April 4, 2012

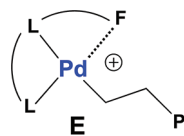
Published: April 24, 2012



Chart 1

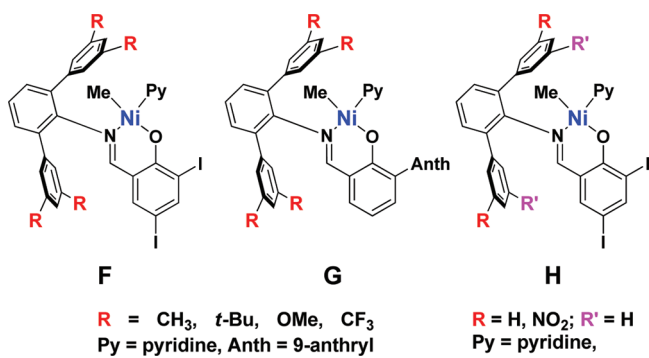


versus the corresponding fluorine-free catalysts.<sup>10</sup> It is thought that the F substituents stabilize 14-electron alkyl intermediates via axial donation to the Pd(II) center (E), thereby suppressing



chain transfer processes involving  $\beta$ -H elimination. These interactions were argued on the basis of <sup>1</sup>H and <sup>19</sup>F NMR spectroscopic data and raise the intriguing question of whether this type or other types of fluorocarbon effects might be more general and might be used to modify chain transfer kinetics in group 10 catalytic systems. In this regard, Mecking's group reported a series of single-component (i.e., no cocatalyst) terphenylphenoxyiminato Ni(II) ethylene polymerization catalysts bearing electron-withdrawing (EWG) or electron-donating groups (EDG) at the terphenyl 3,5-positions (Chart 2, F–H).<sup>3m,p,11</sup>

Chart 2

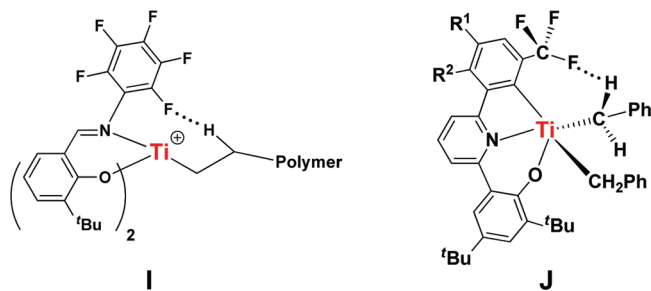


The polymers produced by these catalysts under identical reaction conditions range from high- $M_w$  semicrystalline polyethylenes with low branch densities (EWG substituents) to low- $M_w$  amorphous polyethylenes with high branch densities (EDG substituents). It was suggested that the remote 3',5'-terphenyl substituents impact the polyethylene microstructure via through-bond inductive and/or steric effects, despite their remoteness to the Ni center.<sup>11b,e</sup> It was plausibly suggested that the EWGs afford higher  $M_w$  polyethylenes with lower branch densities by suppressing chain walking and chain transfer relative to chain propagation. Note that catalyst variants bearing a single NO<sub>2</sub> EWG (Chart 2, H) are somewhat less polymerization active than the electron-rich analogues (Chart 2 F,

CH<sub>3</sub> and OCH<sub>3</sub> groups) but exhibit higher thermal stability and yield polyethylenes with comparable  $M_w$  values.<sup>11b,e</sup> Furthermore, in Ni(II) phospho–keto–ylide catalytic systems<sup>12,13</sup> or Ni(II) phenoxyiminato catalysts with an intramolecular hydrogen bond directed toward the active catalytic site,<sup>3c</sup> Ni center electron deficiency significantly enhances ethylene polymerization rates but also enhances branch densities and depresses product  $M_w$  apparently reflecting an interplay of lowered ethylene insertion barriers and enhanced  $\beta$ -agostic interactions.<sup>14</sup>

The introduction of fluorocarbon ligand substituents in group 4 olefin polymerization catalysts has also been associated with changes in enchainment and/or chain transfer kinetics.<sup>15</sup> Fujita reported a series of d<sup>0</sup> group 4 phenoxyiminato catalysts with nonremote fluoro-aryl substitution (Chart 3, e.g., I) that are

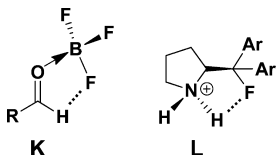
Chart 3. Proposed Ethylene Polymerization Intermediate I and Model Compound J Involving C–H···F–C Interactions



active for the living polymerization of ethylene and propylene. Polymerization activity and  $M_n$  vary widely with the exact aryl substitution pattern, and polymerizations mediated by analogous catalysts without ortho fluorination are no longer living in character and vary greatly in polymerization activity.<sup>16</sup> A C–H···F–C interaction was proposed on the basis of DFT calculations;<sup>16</sup> however, the wide reported variations in activity and  $M_w$  suggest other effects are operative as well. The DFT calculations indicate that the C–F···H–C distances are 2.3–2.4 Å with unexpectedly large<sup>15–17</sup> computed interaction energies of ~7.2 kcal/mol. Experimental evidence for C–H···F–C interactions in neutrally charged d<sup>0</sup> Ti-benzyls is provided by <sup>1</sup>H NMR and neutron diffraction data (Chart 3, J).<sup>17</sup> Here C–H···F–C distances are reported to be 2.572(6) and 2.607(5) Å.

Traditionally, the role that fluorocarbon substituents play in transition-metal homogeneous catalysis has been in inductively tuning catalyst<sup>18</sup> and cocatalyst<sup>19</sup> electronic properties, in stabilizing

catalysts<sup>19</sup> and cocatalysts<sup>20</sup> against electrophilic or free radical attack, in imparting specific stabilization or separation properties to solvents,<sup>18g,21</sup> or in coordinatively screening exposed electrophilic sites, as in structure E. In Lewis acid catalysis, other more subtle secondary interactions such as C—H···F—C hydrogen bonding, arising from the substantial C—F dipole moment,<sup>22</sup> play a role in directing the stereochemical outcome of reactions such as enantioselective aldehyde additions (K, L).<sup>23</sup>



Such interactions are also of great importance in biological systems and play a major role in drug design related substrate–receptor binding in enzymatic catalysis (e.g., Figure 1).<sup>24</sup> These

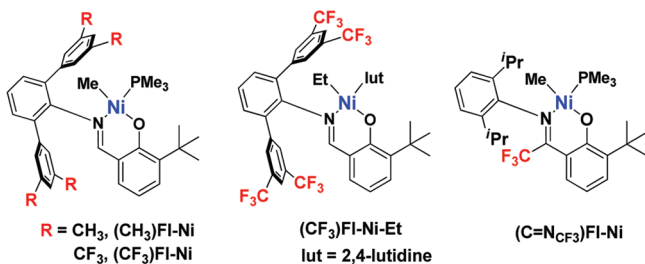


**Figure 1.** Importance of C—H···F—C dipolar interactions in enzymatic substrate–receptor binding: crystal structure (PDB code: 1OYT) showing dipolar C—H···F—C interaction between a fluorinated-tricyclic inhibitor and the enzyme thrombin: C, gray; O, red; N, blue; F, green-yellow. Data are taken from ref 17.

observations raise the question of whether, and to what extent, such interactions might have importance in transition-metal homogeneous catalysis.

In this contribution we focus on the properties of phenoxyiminato Ni(II) ethylene polymerization catalysts ( $\text{CF}_3\text{FI-Ni}$  and  $(\text{CH}_3)\text{FI-Ni}$ ) (Chart 4) activated with the

**Chart 4**



phosphine scavenger/cocatalyst  $\text{Ni}(\text{cod})_2$  and report that introducing *remote* ligand  $\text{CF}_3$  substituents leads to an  $\sim 6.5\times$  increase in polymerization activity and  $66\times$  increase in product  $M_w$  vs those of the fluorine-free analogue. We argue that remote

inductive effects are unlikely to account for this reactivity pattern and propose as an alternative, on the basis of 1D and 2D NMR spectroscopy, X-ray diffraction studies of model compounds, molecular modeling,<sup>25</sup> and reactivity data for catalysts with more proximate  $\text{CF}_3$  groups, that the origin of this remarkable contrast in polymerization characteristics lies primarily in weak secondary F···H interactions between the ligand  $\text{CF}_3$  substituent and the propagating polymer chain, which significantly modify the chain transfer kinetics.

## EXPERIMENTAL SECTION

**Materials and Methods.** All manipulations of air-sensitive materials were performed with rigorous exclusion of  $\text{O}_2$  and moisture in oven-dried Schlenk-type glassware on a dual-manifold Schlenk line, interfaced to a high-vacuum line ( $10^{-6}$  Torr), or in a  $\text{N}_2$ -filled Vacuum Atmospheres glovebox with a high-capacity recirculator (<1 ppm of  $\text{O}_2$ ). Argon (Airgas, prepurified grade) was purified by passage through a supported  $\text{MnO}$  oxygen-removal column and an activated Davison 4A molecular sieve column. Ethylene (Airgas, prepurified grade) was purified by passage through an oxygen/moisture trap (Matheson, Model MTRP-0042-XX). Diethyl ether and tetrahydrofuran were distilled over Na/benzophenone ketyl. Hydrocarbon solvents were vacuum-transferred from Na/K alloy. Benzene- $d_6$  (Cambridge Isotope Laboratories, 99+ atom % D) was stored over Na/K alloy in vacuo and vacuum-transferred immediately prior to use. All other deuterated solvents were used as received (Cambridge Isotope Laboratories, 99+ atom % D). The reagents *trans*- $\text{NiMeCl}(\text{PMe}_3)_2$ ,<sup>25</sup>  $\text{NiCl}_2(2,4\text{-lutidine})_2$ ,<sup>26</sup> 1-*tert*-butyl-2-methoxymethoxybenzene,<sup>27</sup> and the terphenylamines<sup>28</sup> were prepared according to literature procedures.  $\text{Ni}(\text{COD})_2$  (COD = 1,5-cyclooctadiene) was purchased from Strem; all other reagents were purchased from Sigma-Aldrich. The ligands  $(\text{CH}_3)\text{HFI}^{29}$  and  $(\text{CF}_3)\text{HFI}$  were prepared according to literature procedures.<sup>11b</sup>

**Physical and Analytical Measurements.** NMR spectra were recorded on Varian INOVA 400 (400 MHz,  $^1\text{H}$ ; 100 MHz,  $^{13}\text{C}$ ; 162 MHz,  $^{31}\text{P}$ ; 376 MHz,  $^{19}\text{F}$ ), Varian INOVA 500 (500 MHz,  $^1\text{H}$ ), and Bruker AVANCE III 500 (500 MHz,  $^1\text{H}$ ; 125 MHz,  $^{13}\text{C}$ ) NMR spectrometers. Chemical shifts ( $\delta$ ) for  $^1\text{H}$  and  $^{13}\text{C}$  are referenced to TMS, internal solvent resonances are relative to TMS, and the polymer  $\text{CH}_2$  backbone. Chemical shifts ( $\delta$ ) for  $^{31}\text{P}$  and  $^{19}\text{F}$  are referenced to the external standards 85%  $\text{H}_3\text{PO}_4$  and  $\text{CFCl}_3$  dissolved in  $\text{CDCl}_3$ , respectively. NMR spectra of air-sensitive samples were acquired in airtight Teflon valve sealed J. Young NMR tubes. The 2D  $^{19}\text{F}$ ,  $^1\text{H}$  HOESY NMR experiments were carried out on a Bruker AVANCE DRX 400 equipped with a direct QNP probe by setting a relaxation delay of 2 s and a mixing time of 0.8 s. The 2D  $^1\text{H}$ ,  $^1\text{H}$  NOESY NMR experiments were carried out on a Bruker AVANCE III 600 (600 MHz,  $^1\text{H}$ ; 150 MHz  $^{13}\text{C}$ ) with a relaxation delay of 2 s and a mixing time of 0.8 s. The 2D  $^1\text{H}$ ,  $^{13}\text{C}$  HSQC NMR experiments were carried out on a Bruker AVANCE III 600 (600 MHz,  $^1\text{H}$ ; 150 MHz,  $^{13}\text{C}$ ) with a relaxation delay of 1 s. NMR analysis of polymers was carried out in 1,1,2,2-tetrachloroethane- $d_2$  at 120 °C with  $d_1 = 10$  s. Polymer NMR spectra were assigned and polyethylene branch numbers calculated according to standard literature procedures for polyethylene.<sup>30</sup> Gel permeation chromatography (GPC) was carried out in 1,2,4-trichlorobenzene (stabilized with 125 ppm of BHT) at 150 °C on a Polymer Laboratories 220 instrument equipped with a set of three PLgel 10 μm mixed-B LS columns with differential refractive index and viscosity detectors. Molecular weights were determined by Universal Calibration relative to polystyrene standards. Elemental analyses were conducted by Midwest Microlab, Indianapolis, IN.

**Synthesis of *N*-(2,6-Diisopropylphenyl)-2,2,2-trifluoroacetylmidoyl Chloride (1).** The general procedure of Uneyama<sup>31</sup> was followed with the following modifications. A 500 mL flask was charged with  $\text{Ph}_3\text{P}$  (34 g, 132 mmol),  $\text{Et}_3\text{N}$  (7.3 mL, 53 mmol), and  $\text{CCl}_4$  (21.1 mL, 220 mmol). The mixture was stirred at 0 °C for 30 min. Trifluoroacetic acid (5.0 mL, 65 mmol) was then added via syringe and the reaction mixture stirred at 0 °C for another 30 min. A mixture of 2,6-diisopropylaniline (1.0 mL, 53 mmol) and  $\text{CCl}_4$  (21.1 mL,

220 mmol) was then added, and the mixture was warmed to room temperature and stirred for 30 min. The mixture was then refluxed with stirring for an additional 3 h. All the volatiles were removed under vacuum, and the residue was diluted with hexanes and filtered. The volatiles were next removed from the filtrate in vacuo, yielding a yellow oil which was purified by column chromatography on silica gel with 15/1 hexane/ethyl acetate as the eluent to give **1** as a colorless oil (11.5 g, 90% yield). The <sup>1</sup>H NMR spectrum was in good agreement with that reported by Boere.<sup>32</sup>

**Synthesis of (2-Methoxymethoxy-3-tert-butylphenyl)-lithium-TMEDA (2).** A 500 mL flask was charged with *n*-BuLi (36.0 mL, 90.0 mmol), TMEDA (13.4 mL, 90.0 mmol), and 100 mL of diethyl ether at 0 °C. To this solution was added dropwise 1-*tert*-butyl-2-methoxymethoxybenzene (17.0 g, 87.5 mmol) in diethyl ether at 0 °C over a period of 2 h. The resulting mixture was stirred at 0 °C for 2 h and then at room temperature overnight. All the volatiles were then removed, and the resulting dark solid was washed with pentane (250 mL × 3). The solid was then dried under vacuum to yield a white solid (20.6 g, 75% yield). <sup>1</sup>H NMR (*THF-d*<sub>8</sub>, 500 MHz): δ 7.47 (d, *J* = 7 Hz, 1H, Ar H), 6.72 (d, *J* = 7 Hz, 1H, Ar H), 6.55 (t, *J* = 7 Hz, 1H, Ar H), 5.43 (s, 2H, OCH<sub>2</sub>O), 3.42 (s, 3H, OCH<sub>3</sub>), 2.31 (s, 4H, NCH<sub>2</sub>), 2.16 (s, 12H, NCH<sub>3</sub>), 1.36 (s, 9H, C(CH<sub>3</sub>)<sub>3</sub>) ppm. <sup>13</sup>C NMR (*THF-d*<sub>8</sub>, 125 MHz): δ 166.6, 141.8, 132.4, 121.8, 121.2, 92.7 (OCH<sub>2</sub>O), 59.1 (OCH<sub>3</sub>), 54.9 (NCH<sub>2</sub>), 46.4 (NCH<sub>3</sub>), 35.1 (C(CH<sub>3</sub>)<sub>3</sub>), 31.2 (C(CH<sub>3</sub>)<sub>3</sub>) ppm.

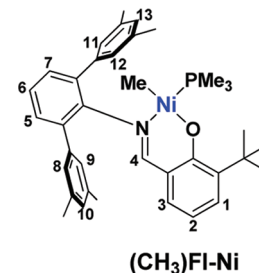
**Synthesis of 2-*tert*-Butyl-6-(2,2,2-trifluoro-1-(2,6-diisopropylphenyl)iminoethyl)(methoxymethoxy)benzene (3).** A 200 mL flask was charged with **2** (2.29 g, 7.24 mmol) and 60 mL of diethyl ether at 0 °C. Next, **1** (2.10 g, 7.24 mmol) in 30 mL of diethyl ether was added by addition funnel over 30 min at 0 °C. The mixture was stirred at 0 °C for 3 h and then at room temperature for 6 h. Water (50 mL) was then added, the organic layer was separated, dried over Na<sub>2</sub>SO<sub>4</sub>, and filtered, and the filtrate was evaporated to yield a brown solid. The solid was recrystallized from methanol, affording 2.66 g of **3** (82% yield). <sup>1</sup>H NMR (*C<sub>2</sub>D<sub>2</sub>Cl<sub>4</sub>*, 120 °C, 400 MHz): δ 7.58 (d, *J* = 8 Hz, 1H, Ar H), 7.44 (d, *J* = 8 Hz, 1H, Ar H), 7.00 (br, 4H, Ar H), 4.12 (s, 2H, OCH<sub>2</sub>O), 3.05 (s, 3H, OCH<sub>3</sub>), 2.88 (septa, *J* = 6 Hz, 2H, CH(CH<sub>3</sub>)<sub>2</sub>), 1.05 (d, *J* = 6 Hz, 12H, CH(CH<sub>3</sub>)<sub>2</sub>), 1.04 (s, 9H, C(CH<sub>3</sub>)<sub>3</sub>) ppm. GC-MS: *m/z* 449 (M<sup>+</sup>).

**Synthesis of 2-*tert*-Butyl-6-(2,2,2-trifluoro-1-(2,6-diisopropylphenyl)iminoethyl)phenol ((C=N<sub>CF<sub>3</sub></sub>)HFI).** A 100 mL flask was charged with **3** (2.66 g), CH<sub>2</sub>Cl<sub>2</sub> (30 mL), and concentrated HCl (20 mL). The mixture was then stirred at room temperature for 6 h. Water (50 mL) was next added, the organic layer was separated, dried over Na<sub>2</sub>SO<sub>4</sub>, and filtered, and the filtrate was evaporated to dryness, affording (C=N<sub>CF<sub>3</sub></sub>)HFI as a red oil (2.06 g, 95% yield). <sup>1</sup>H NMR (*CDCl<sub>3</sub>*, 500 MHz): δ 14.10 (s, 1H, OH), 7.65 (d, *J* = 7 Hz, 1H, Ar H), 7.52 (d, *J* = 7 Hz, 1H, Ar H), 7.21–7.16 (m, 3H, Ar H), 6.92 (t, *J* = 7 Hz, 1H, Ar H), 2.73 (septa, *J* = 7 Hz, 2H, CH(CH<sub>3</sub>)<sub>2</sub>), 1.48 (s, 9H, C(CH<sub>3</sub>)<sub>3</sub>), 1.20 (d, *J* = 7 Hz, 6H, CH(CH<sub>3</sub>)<sub>2</sub>), 1.17 (d, *J* = 7 Hz, 6H, CH(CH<sub>3</sub>)<sub>2</sub>) ppm. <sup>13</sup>C NMR (*CDCl<sub>3</sub>*, 125 MHz): δ 162.8, 141.6, 139.0, 135.5 (d, <sup>2</sup>J<sub>CF</sub> = 30 Hz, CF<sub>3</sub>C=N), 131.8, 127.5 (d, <sup>1</sup>J<sub>CF</sub> = 290.0 Hz, CF<sub>3</sub>), 125.2, 123.2, 119.9, 117.9, 117.6, 113.6, 35.4 (C(CH<sub>3</sub>)<sub>3</sub>) 29.5 (C(CH<sub>3</sub>)<sub>3</sub>), 28.7 (CH(CH<sub>3</sub>)<sub>2</sub>), 23.8 (CH(CH<sub>3</sub>)<sub>2</sub>), 22.8 (CH(CH<sub>3</sub>)<sub>2</sub>) ppm. <sup>19</sup>F NMR (*CDCl<sub>3</sub>*, 376 MHz): δ -59.7 (d, <sup>1</sup>J<sub>CF</sub> = 3 Hz) ppm. GC-MS: *m/z* 405 (M<sup>+</sup>).

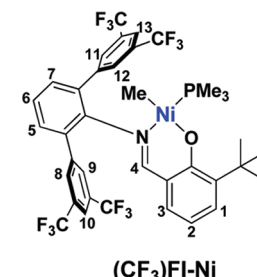
**Representative Procedure for the Synthesis of Sodium Salts (CH<sub>3</sub>)FI-Na, (CF<sub>3</sub>)FI-Na, and (C=N<sub>CF<sub>3</sub></sub>)FI-Na.** Under N<sub>2</sub>, a 100 mL Schlenk flask was charged with 0.902 g (1.33 mmol) of (CF<sub>3</sub>)HFI and 0.080 g (3.33 mmol) of NaH. To this was added 75 mL of dry THF via syringe. This red-orange mixture was stirred for 24 h. The reaction mixture was then filtered, and the volatiles were removed in vacuo. The resulting bright yellow solid was dried under high vacuum overnight and was used without purification in the synthesis of (CF<sub>3</sub>)FI-Ni.

**Synthesis of [2-*tert*-Butyl-6-((2,6-(3,5-dimethylphenyl)-phenylimino)methyl)phenolato]nickel(II) Methyl Trimethylphosphine ((CH<sub>3</sub>)FI-Ni).** A 100 mL Schlenk flask was charged with 0.740 g (1.53 mmol) of (CH<sub>3</sub>)FI-Na, 0.399 g (1.53 mmol) of *trans*-NiMeCl(PMe<sub>3</sub>)<sub>2</sub>, and 45 mL of dry benzene. The resulting red-orange reaction mixture was then stirred at room temperature for 6 h. The

mixture was then filtered, and the volatiles were removed from the filtrate under vacuum, affording 0.695 g (1.14 mmol, 75% yield) of orange solid. Crystals suitable for X-ray analysis were obtained by slowly cooling an *n*-hexane/toluene solution of (CH<sub>3</sub>)FI-Ni under N<sub>2</sub>. Anal. Calcd for C<sub>37</sub>H<sub>46</sub>NNiOP: C, 72.80; H, 7.60; N, 2.29. Found: C, 72.63; H, 7.74; N, 2.18. <sup>1</sup>H NMR (C<sub>6</sub>D<sub>6</sub>, 500 MHz): δ 7.86 (s, 1H, 4-H), 7.29 (m, 5H, 1-, 8-, 9-, 11-, and 12-H), 7.18–7.12 (m, 3H, 1-, 2-, and 3-H), 6.76 (s, 2H, 10- and 13-H), 6.69 (dd, <sup>3</sup>J<sub>HH</sub> = 7.8 Hz, <sup>4</sup>J<sub>HH</sub> = 1.9 Hz, 1H, 3-H), 6.42 (t, <sup>3</sup>J<sub>HH</sub> = 7.5 Hz, 1H, 2-H), 2.13 (s, 12H, Ar CH<sub>3</sub>), 1.41 (s, 9H, 'Bu), 0.73 (d, <sup>2</sup>J<sub>PH</sub> = 9.5 Hz, 9H, P(CH<sub>3</sub>)<sub>3</sub>), -0.98 (s, 3H, Ni-CH<sub>3</sub>) ppm. <sup>13</sup>C NMR (C<sub>6</sub>D<sub>6</sub>, 125 MHz): δ 168.45, 166.67, 149.92, 141.02, 140.66, 137.56, 137.27, 133.29, 130.84, 130.47, 128.98, 128.79, 128.35, 125.71, 120.76, 113.02, 35.26, 29.74, 21.51, 13.58, 13.48 (d, <sup>1</sup>J<sub>CP</sub> = 25.8 Hz, P(CH<sub>3</sub>)<sub>3</sub>), -13.68 (d, <sup>2</sup>J<sub>CP</sub> = 30.9 Hz, Ni-CH<sub>3</sub>) ppm. <sup>31</sup>P NMR (C<sub>6</sub>D<sub>6</sub>, 162 MHz): δ -13.8 ppm.

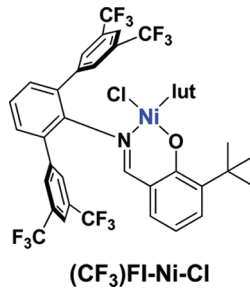


**Synthesis of [2-*tert*-Butyl-6-((2,6-(3,5-bis(trifluoromethyl)phenyl)phenylimino)methyl)phenolato]nickel(II) Methyl Trimethylphosphine ((CF<sub>3</sub>)FI-Ni).** A 100 mL Schlenk flask was charged with 0.489 g (0.699 mmol) of (CF<sub>3</sub>)FI-Na, 0.183 g (0.700 mmol) of *trans*-NiMeCl(PMe<sub>3</sub>)<sub>2</sub>, and 35 mL of dry benzene. The resulting red reaction mixture was stirred at room temperature for 6 h. The mixture was then filtered, and the volatiles were removed from the filtrate under high vacuum, affording 0.320 g (0.387 mmol, 55% yield) of a red-orange solid. Crystals suitable for X-ray analysis were obtained by cooling an *n*-hexane/toluene solution of (CF<sub>3</sub>)FI-Ni under N<sub>2</sub>. Anal. Calcd for C<sub>37</sub>H<sub>34</sub>NF<sub>12</sub>NiOP: C, 53.78; H, 4.15; N, 1.70. Found: C, 54.00; H, 4.08; N, 1.81. <sup>1</sup>H NMR (C<sub>6</sub>D<sub>6</sub>, 500 MHz): δ 8.03 (s, 4H, 8-, 9-, 11-, and 12-H), 7.67 (s, 2H, 10- and 13-H), 7.21 (dd, <sup>3</sup>J<sub>HH</sub> = 7.3 Hz, <sup>4</sup>J<sub>HH</sub> = 1.8 Hz, 1H, 1-H), 7.18 (d, 1H, 4-H), 6.99–6.91 (m, 3H, 5-, 6-, and 7-H), 6.48 (dd, <sup>3</sup>J<sub>HH</sub> = 7.9 Hz, <sup>4</sup>J<sub>HH</sub> = 1.9 Hz, 1H, 3-H), 6.37 (t, <sup>3</sup>J<sub>HH</sub> = 7.4 Hz, 1H, 2-H), 1.33 (s, 9H, 'Bu), 0.70 (d, <sup>2</sup>J<sub>PH</sub> = 9.7 Hz, 9H, P(CH<sub>3</sub>)<sub>3</sub>), -1.33 (d, <sup>3</sup>J<sub>PH</sub> = 7.6 Hz, 3H, Ni-CH<sub>3</sub>) ppm. <sup>13</sup>C NMR (C<sub>6</sub>D<sub>6</sub>, 125 MHz): δ 168.18, 167.27, 150.46, 141.93, 140.76, 133.94, 132.95, 131.91, 131.63, 131.36, 131.10, 130.72, 127.72, 126.22, 123.82 (q, <sup>1</sup>J<sub>CF</sub> = 274.2 Hz, CF<sub>3</sub>), 120.86, 119.07, 113.87, 34.92, 29.44, 13.24 (d, <sup>1</sup>J<sub>CP</sub> = 27.6 Hz, P(CH<sub>3</sub>)<sub>3</sub>), -13.48 (d, <sup>2</sup>J<sub>CP</sub> = 44.7 Hz, Ni-CH<sub>3</sub>) ppm. <sup>31</sup>P NMR (C<sub>6</sub>D<sub>6</sub>, 162 MHz): δ -12.56 ppm. <sup>19</sup>F NMR (C<sub>6</sub>D<sub>6</sub>, 376 MHz): δ -62.92 ppm.

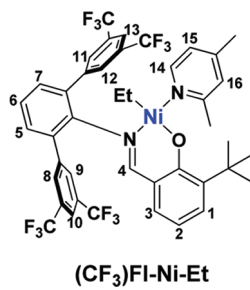


**Synthesis of [2-*tert*-Butyl-6-((2,6-(3,5-bis(trifluoromethyl)phenyl)phenylimino)methyl)phenolato]nickel(II) Chloro (2,4-Lutidine ((CF<sub>3</sub>)FI-Ni-Cl)).** A 100 mL Schlenk flask was charged with 0.930 g (1.33 mmol) of (CF<sub>3</sub>)FI-Na. THF (30 mL) was added, and the resulting yellow solution was transferred slowly via cannula over 20 min to a flask containing 0.458 g (1.33 mmol) of NiCl<sub>2</sub>(2,4-lutidine)<sub>2</sub> and 15 mL of THF. An immediate color change to dark red was

observed, and the reaction mixture was stirred for 90 min at room temperature. The volatiles were then removed in vacuo, leaving a dark orange oil. Dichloromethane (35 mL) was added, and the reaction mixture was filtered. The filtrate was concentrated in vacuo, and pentane (40 mL) was added. The reaction mixture was then cooled to  $-40^{\circ}\text{C}$  overnight, upon which a yellow-brown solid precipitated from solution. This solid was isolated via filtration at  $-78^{\circ}\text{C}$ , and the resulting microcrystalline solid was dried under high vacuum, affording 0.632 g (0.720 mmol, 54%) of paramagnetic  $(\text{CF}_3)\text{FI-Ni-Cl}$ .<sup>33</sup>

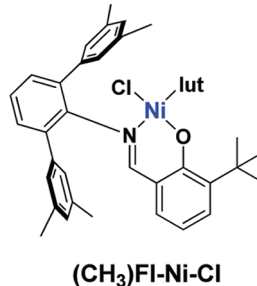


**Synthesis of [2-*tert*-Butyl-6-((2,6-(3,5-bis(trifluoromethyl)phenyl)phenylimino)methyl)phenolato]nickel(II) Ethyl 2,4-Lutidine ((CF<sub>3</sub>)FI-Ni-Et).** A 50 mL Schlenk flask was charged with 0.568 g (0.647 mmol) of  $(\text{CF}_3)\text{FI-Ni-Cl}$  and ether (30 mL). The reaction flask was cooled to  $-78^{\circ}\text{C}$ , and ethylmagnesium chloride (2.0 M, 0.57 mL, 1.14 mmol) was added dropwise. The reaction mixture was stirred at  $-78^{\circ}\text{C}$  for 2 h and then stirred at  $-42^{\circ}\text{C}$  for 1 h. The orange-red mixture was next warmed to room temperature and filtered. The orange-red reaction mixture was then warmed to room temperature and filtered, and the filtrate was concentrated in vacuo. Dry *n*-pentane (30 mL) was then added via syringe, precipitating an orange solid. After filtration and drying under high vacuum, 0.360 g (0.549 mmol, 48%) of  $(\text{CF}_3)\text{FI-Ni-Et}$  was isolated. <sup>1</sup>H NMR ( $\text{C}_6\text{D}_6$ , 500 MHz):  $\delta$  8.68 (d,  $J = 5.5$  Hz, 1H), 7.66 (s, 1H), 7.59 (s, 2H), 7.47–7.36 (m, 4H), 7.15 (d,  $J = 8.2$  Hz, 4H), 6.90 (s, 2H), 6.69 (d,  $J = 7.4$  Hz, 1H), 6.31 (t,  $J = 7.4$  Hz, 1H), 6.26 (s, 1H), 6.16 (d,  $J = 4.6$  Hz, 1H), 3.14 (s, 3H), 2.29 (d,  $J = 16.6$  Hz, 12H), 1.57 (s, 3H), 1.02 (s, 9H), 0.32–0.14 (m, 2H), 0.04 (t,  $J = 7.4$  Hz, 3H) ppm. <sup>13</sup>C NMR ( $\text{C}_6\text{D}_6$ , 125 MHz):  $\delta$  169.28, 166.58, 159.60, 150.86, 149.69, 146.78, 140.65, 140.55, 137.45, 137.16, 136.82, 132.65, 130.25, 130.15, 129.08, 128.82, 125.79, 124.76, 121.34, 120.40, 112.61, 34.62, 29.34, 25.31, 21.68, 21.61, 20.21, 16.07, 1.61 ppm. <sup>19</sup>F NMR ( $\text{C}_6\text{D}_6$ , 376 MHz):  $\delta$  -62.78, -62.95 ppm.

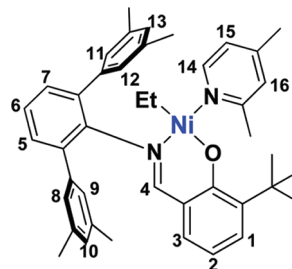


**Synthesis of [2-*tert*-Butyl-6-((2,6-(3,5-dimethylphenyl)phenylimino)methyl)phenolato]nickel(II) Chloro 2,4-Lutidine ((CH<sub>3</sub>)FI-Ni-Cl).** A 100 mL Schlenk flask was charged with 2.10 g (4.35 mmol) of  $(\text{CH}_3)\text{FI-Na}$ . THF (50 mL) was added, and the resulting yellow solution was transferred slowly via cannula over 20 min to a flask containing 1.50 g (4.36 mmol) of  $\text{NiCl}_2(2,4\text{-lutidine})_2$  and 25 mL of THF. An immediate color change to dark red was observed, and the reaction mixture was stirred for 90 min at room temperature. The volatiles were then removed in vacuo, leaving a dark orange oil. Dichloromethane (50 mL) was added, and the reaction mixture was filtered. The filtrate was concentrated in vacuo, and pentane (50 mL) was added, precipitating a brown solid. This solid was isolated via

filtration, and the resulting solid was dried under high vacuum, affording 2.012 g (3.04 mmol, 70%) of paramagnetic  $(\text{CH}_3)\text{FI-Ni-Cl}$ .<sup>33</sup>

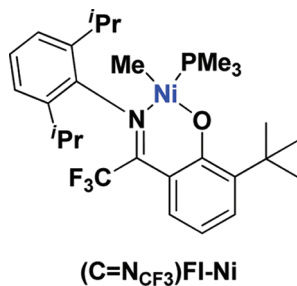


**Synthesis of [2-*tert*-Butyl-6-((2,6-(3,5-dimethylphenyl)phenylimino)methyl)phenolato]nickel(II) Ethyl 2,4-Lutidine ((CH<sub>3</sub>)FI-Ni-Et).** A 100 mL Schlenk flask was charged with 0.749 g (1.13 mmol) of  $(\text{CH}_3)\text{FI-Ni-Cl}$  and ether (50 mL). The reaction flask was cooled to  $-78^{\circ}\text{C}$ , and ethylmagnesium chloride (2.0 M, 0.57 mL, 1.14 mmol) was added dropwise. The reaction mixture was stirred at  $-78^{\circ}\text{C}$  for 2 h and then stirred at  $-42^{\circ}\text{C}$  for 1 h. The orange-red mixture was next warmed to room temperature and filtered. The orange-red reaction mixture was then warmed to room temperature and filtered, and the filtrate was concentrated in vacuo. Dry *n*-pentane (30 mL) was then added via syringe, precipitating an orange solid. After filtration and drying under high vacuum, 0.360 g (0.549 mmol, 48%) of  $(\text{CH}_3)\text{FI-Ni-Et}$  was isolated. <sup>1</sup>H NMR ( $\text{C}_6\text{D}_6$ , 500 MHz):  $\delta$  8.68 (d,  $J = 5.5$  Hz, 1H), 7.66 (s, 1H), 7.59 (s, 2H), 7.47–7.36 (m, 4H), 7.15 (d,  $J = 8.2$  Hz, 4H), 6.90 (s, 2H), 6.69 (d,  $J = 7.4$  Hz, 1H), 6.31 (t,  $J = 7.4$  Hz, 1H), 6.26 (s, 1H), 6.16 (d,  $J = 4.6$  Hz, 1H), 3.14 (s, 3H), 2.29 (d,  $J = 16.6$  Hz, 12H), 1.57 (s, 3H), 1.02 (s, 9H), 0.32–0.14 (m, 2H), 0.04 (t,  $J = 7.4$  Hz, 3H) ppm. <sup>13</sup>C NMR ( $\text{C}_6\text{D}_6$ , 125 MHz):  $\delta$  169.28, 166.58, 159.60, 150.86, 149.69, 146.78, 140.65, 140.55, 137.45, 137.16, 136.82, 132.65, 130.25, 130.15, 129.08, 128.82, 125.79, 124.76, 121.34, 120.40, 112.61, 34.62, 29.34, 25.31, 21.68, 21.61, 20.21, 16.07, 1.61 ppm.



**Synthesis of [2-*tert*-Butyl-6-(2,2,2-trifluoro-1-(2,6-diisopropylphenyl)iminoethyl)phenolato]nickel(II) Methyl Tri-methylphosphine ((C=N<sub>CF<sub>3</sub></sub>)FI-Ni).** A 100 mL Schlenk flask was charged with 0.521 g of  $(\text{C}=\text{N}_{\text{CF}_3})\text{FI-Na}$  (1.04 mmol), 0.273 g of *trans*- $\text{NiMeCl}(\text{PMe}_3)_2$  (1.04 mmol), and 45 mL of dry benzene. The resulting red-orange reaction mixture was stirred at room temperature for 6 h. The mixture was then filtered, and the volatiles were removed from the filtrate under high vacuum, affording 0.528 g (91% yield) of a red solid. Crystals suitable for X-ray analysis were obtained by slowly cooling an *n*-hexane/toluene solution of  $(\text{C}=\text{N}_{\text{CF}_3})\text{FI-Ni}$  under  $\text{N}_2$ . Anal. Calcd for  $\text{C}_{37}\text{H}_{46}\text{NNiOP}$ : C, 60.67; H, 7.46; N, 2.53. Found: C, 61.62; H, 7.30; N, 2.30. <sup>1</sup>H NMR ( $\text{C}_6\text{D}_6$ , 500 MHz):  $\delta$  7.75 (d,  $J = 7$  Hz, 1H, Ar H), 7.38 (d,  $J = 7$  Hz, 1H, Ar H), 7.11–7.06 (m, 3H, Ar H), 6.58 (t,  $J = 7$  Hz, 1H, Ar H), 4.10 (septa,  $J = 7$  Hz, 2H,  $\text{CH}(\text{CH}_3)_2$ ), 1.52 (d,  $J = 7$  Hz, 6H,  $\text{CH}(\text{CH}_3)_2$ ), 1.46 (s, 9H,  $\text{C}(\text{CH}_3)_3$ ), 0.84 (d,  $J = 7$  Hz, 6H,  $\text{CH}(\text{CH}_3)_2$ ), 0.84 (d,  $J_{\text{PH}} = 10$  Hz, 9H,  $\text{P}(\text{CH}_3)_3$ ), -1.41 (d,  $J = 6$  Hz, 3H,  $\text{Ni-CH}_3$ ) ppm. <sup>13</sup>C NMR ( $\text{C}_6\text{D}_6$ , 125 MHz):  $\delta$  169.0, 146.1, 142.0, 139.6, 131.2, 128.7, 126.6, 124.1, 123.9, 122.1, 120.7, 113.7, 36.0 ( $\text{C}(\text{CH}_3)_3$ ), 31.0 ( $\text{C}(\text{CH}_3)_3$ ), 29.6 ( $\text{CH}(\text{CH}_3)_2$ ), 25.7 ( $\text{CH}(\text{CH}_3)_2$ ),

25.0 ( $\text{CH}(\text{CH}_3)_2$ ), 14.9 ( $\text{P}(\text{CH}_3)_3$ ), -11.5 ( $\text{Ni}-\text{CH}_3$ ) ppm.  $^{31}\text{P}$  NMR ( $\text{C}_6\text{D}_6$ , 162 MHz):  $\delta$  -14.8 ppm.  $^{19}\text{F}$  NMR ( $\text{C}_6\text{D}_6$ , 376 MHz):  $\delta$  -53.0 ppm.



**General Procedure for Ethylene Polymerization Experiments.** In a typical experiment, an oven-dried 350 mL glass thick-walled pressure vessel was charged in the glovebox with 5  $\mu\text{mol}$  of Ni catalyst, 2.0 equiv of  $\text{Ni}(\text{COD})_2$ , 50 mL of dry toluene, and a large magnetic stir bar. The pressure vessel was then interfaced to a high-pressure line, and the solution was degassed. The reactor was warmed to the desired temperature using a water or oil bath and allowed to equilibrate for 5 min. With rapid stirring, the reactor was then pressurized to 8.0 atm of ethylene, which was maintained during the course of the polymerization. After the desired run time, the reactor was vented and the contents poured into acidic methanol (10%). The precipitated polymer was collected by filtration, washed with methanol, and dried at 60 °C overnight under high vacuum.

**Molecular Modeling Calculations.** Molecular modeling was performed with semiempirical and ab initio codes included in the Spartan 06 software package.<sup>34</sup> Preoptimization was performed at the PM3 semiempirical level,<sup>35</sup> and Hartree-Fock (HF) ab initio calculations were carried out using 6-31G\*\* basis sets to find the equilibrium geometry in the ground state for catalysts  $(\text{CF}_3)\text{FI-Ni}$  and  $(\text{CH}_3)\text{FI-Ni}$  with an *n*-butyl group modeling the polyethylene chain. Restriction to a square-planar geometry was applied at the Ni center. In the semiempirical and ab initio calculations, the gradient norms were  $10^{-4}$  hartree/Bohr and 0.05 kcal/Å, respectively.

**X-ray Crystal Structure Determinations for  $(\text{CH}_3)\text{FI-Ni}$ ,  $(\text{CF}_3)\text{FI-Ni}$ ,  $(\text{CF}_3)\text{FI-Ni-Et}$ , and  $(\text{C=N}_{\text{CF}_3})\text{FI-Ni}$ .** Intensity data for  $(\text{CH}_3)\text{FI-Ni}$ ,  $(\text{CF}_3)\text{FI-Ni}$ ,  $(\text{CF}_3)\text{FI-Ni-Et}$ , and  $(\text{C=N}_{\text{CF}_3})\text{FI-Ni}$  were collected at -173 °C on a Bruker AXS APEXII diffractometer equipped with a CCD area detector using graphite-monochromated Mo  $\text{K}\alpha$  ( $\lambda = 0.7107 \text{ \AA}$ ,  $(\text{CF}_3)\text{FI-Ni-Et}$  and  $(\text{C=N}_{\text{CF}_3})\text{FI-Ni}$ ) or Cu  $\text{K}\alpha$  ( $\lambda = 1.5418 \text{ \AA}$ ,  $(\text{CH}_3)\text{FI-Ni}$  and  $(\text{CF}_3)\text{FI-Ni}$ ) radiation. All data were corrected for absorption using an empirical correction. Structure solutions and refinements were obtained by SIR-92,<sup>36</sup> SHELXS-97,<sup>37</sup> or OLEX2<sup>38</sup> using direct methods and were refined on  $F^2$  using full-matrix least-squares techniques. All hydrogen atoms were refined with a riding model. All non-hydrogen atoms were refined anisotropically. Crystals of  $(\text{CH}_3)\text{FI-Ni}$  were found to be nonmerohedrally twinned. The data were processed using both orientation matrices identified by the program Cell\_Now.<sup>39</sup> The remaining structures were solved and refined routinely. In  $(\text{CF}_3)\text{FI-Ni-Et}$ , significant disorder (70%/30%) exists in the Ni-ethyl conformation and fluorine atoms F10, F11, and F12 (80/20%). Distance restraints for equivalent bonds were refined for the disordered ethyl and  $\text{CF}_3$  groups. Rigid bond restraints were imposed on the displacement parameters as well as restraints on similar amplitudes separated by less than 1.7 Å on disordered atoms. Crystallographic results are summarized in Table S2 of the Supporting Information, and displacement ellipsoid plots for  $(\text{CF}_3)\text{FI-Ni}$ ,  $(\text{CH}_3)\text{FI-Ni}$ ,  $(\text{CF}_3)\text{FI-Ni-Et}$ , and  $(\text{C=N}_{\text{CF}_3})\text{FI-Ni}$  are shown in Figures 2-5, respectively.

## RESULTS

A primary goal of this study is to investigate the effects of installing remote fluorocarbon substituents on phenoxyiminato-based Ni(II) ethylene polymerization catalysts. It will be seen

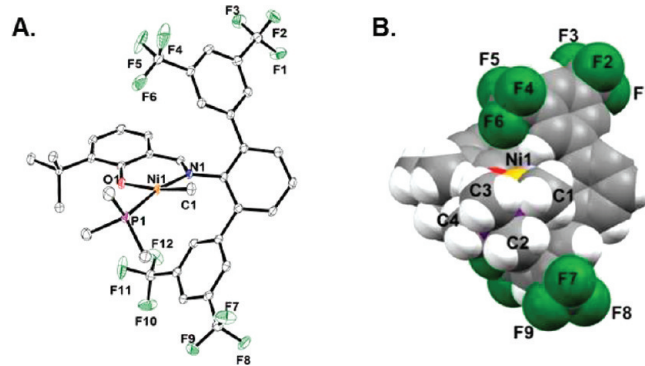


**Figure 2.** (A) Displacement ellipsoid plot (50%) of precatalyst complex  $(\text{CF}_3)\text{FI-Ni}$ . H atoms are omitted for clarity. Selected bond distances (Å) and angles (deg): Ni—C1, 1.953(2); Ni—P1, 2.1496(6); Ni—N1, 1.936(2); Ni—O1, 1.914(1); Ni···F6, 4.299(2);  $\angle \text{N1-Ni-C1}$ , 92.46(8);  $\angle \text{C1-Ni-P1}$ , 84.71(6);  $\angle \text{P1-Ni-O1}$ , 92.46(4);  $\angle \text{O1-Ni-N1}$ , 92.35(6);  $\angle \text{N1-Ni-C1}$ , 92.46(8);  $\angle \text{N1-Ni-P1}$ , 169.03(5);  $\angle \text{O1-Ni-C1}$ , 168.26(8). (B) Space-filling model of  $(\text{CF}_3)\text{FI-Ni}$ : Ni, orange; F, green; C, gray; P, purple; O, red; H, white.

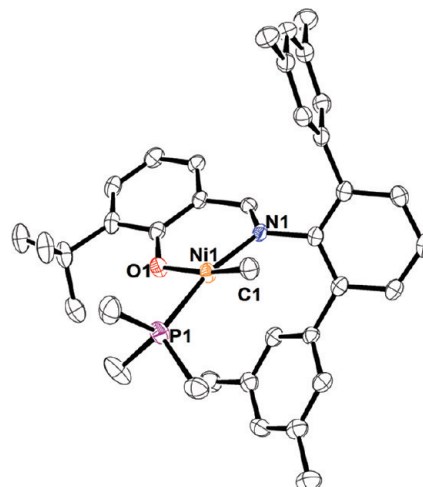


**Figure 3.** Displacement ellipsoid plot (50%) of precatalyst  $(\text{CH}_3)\text{FI-Ni}$ . H atoms and solvent molecules are omitted for clarity. Selected bond distances (Å) and angles (deg): Ni—C1, 1.937(3); Ni—P1, 2.1420(9); Ni—N1, 1.937(2); Ni—O1, 1.917(2);  $\angle \text{N1-Ni-C1}$ , 91.7(1);  $\angle \text{C1-Ni-P1}$ , 85.7(1);  $\angle \text{P1-Ni-O1}$ , 92.29(7);  $\angle \text{O1-Ni-N1}$ , 92.70(9);  $\angle \text{N1-Ni-C1}$ , 91.7(1);  $\angle \text{N1-Ni-P1}$ , 168.05(7);  $\angle \text{O1-Ni-C1}$ , 167.5(1).

that introducing remote  $\text{CF}_3$  substituents in these Ni(II) catalysts has dramatic effects on catalyst activity, thermal stability, and product polyolefin molecular weight characteristics. These differences in polymerization properties are attributed primarily to C—F···H—C interactions between the remote  $\text{CF}_3$  substituent and a H atom on the  $\beta$ -carbon of the growing polyethylene chain which conformationally impedes chain transfer.

**Catalyst Synthesis.** The phenoxyiminato ligands employed in this study were prepared following generalizable literature procedures.<sup>11b</sup> The sodium salts of  $(\text{CH}_3)\text{HFI}$  and  $(\text{CF}_3)\text{HFI}$  were prepared by stirring the free ligands with excess NaH in THF (Scheme 1). The neutrally charged Ni(II) catalysts  $(\text{CH}_3)\text{FI-Ni}$  and  $(\text{CF}_3)\text{FI-Ni}$  were then prepared by stirring the sodium salts with 1 equiv of *trans*- $\text{NiClMe}(\text{PMe}_3)_2$  in benzene (Scheme 1). The constitutions and structures of

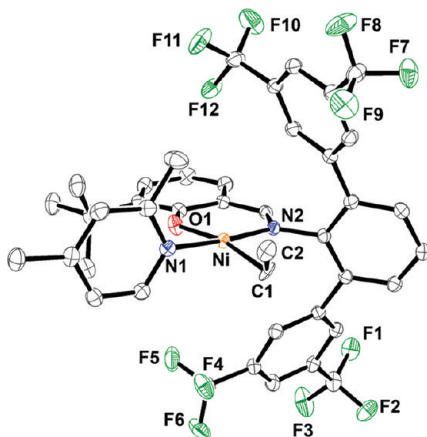


**Figure 4.** Displacement ellipsoid plot (50%) of the 70% Ni-Et conformer of complex  $(CF_3)FI\text{-}Ni\text{-Et}$ . H atoms are omitted for clarity. Selected distances ( $\text{\AA}$ ) and angles (deg): Ni–C1, 2.017(5); Ni–N1, 1.914(1); Ni–N2, 1.893(1); Ni–O1, 1.893(1); C2–H2…F9, 3.66(2); Ni…F4, 4.113(2); Ni…F12, 4.412(2);  $\angle N2\text{-Ni-C1}$ , 96.57(19);  $\angle C1\text{-Ni-N1}$ , 88.17(19);  $\angle N1\text{-Ni-O1}$ , 82.74(6);  $\angle O1\text{-Ni-N2}$ , 93.04(6);  $\angle O1\text{-Ni-C1}$ , 166.97(18).

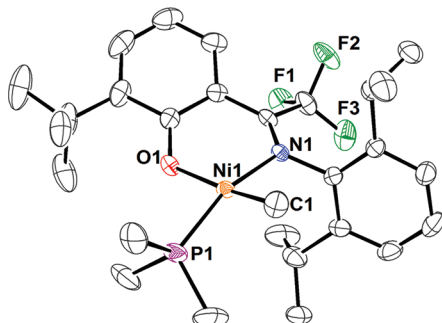


**Figure 5.** Displacement ellipsoid plot (50%) of precatalyst complex  $(C=NCF_3)FI\text{-Ni}$ . H atoms are omitted for clarity. Selected bond distances ( $\text{\AA}$ ) and angles (deg): Ni–C1, 1.931(2); Ni–P1, 2.1353(5); Ni–N1, 1.968(1); Ni–O1, 1.900(1);  $\angle N1\text{-Ni-C1}$ , 94.04(7);  $\angle C1\text{-Ni-P1}$ , 85.42(6);  $\angle P1\text{-Ni-O1}$ , 92.68(4);  $\angle O1\text{-Ni-N1}$ , 91.86(6);  $\angle N1\text{-Ni-C1}$ , 94.04(7);  $\angle N1\text{-Ni-P1}$ , 161.87(5);  $\angle O1\text{-Ni-C1}$ , 166.57(8).

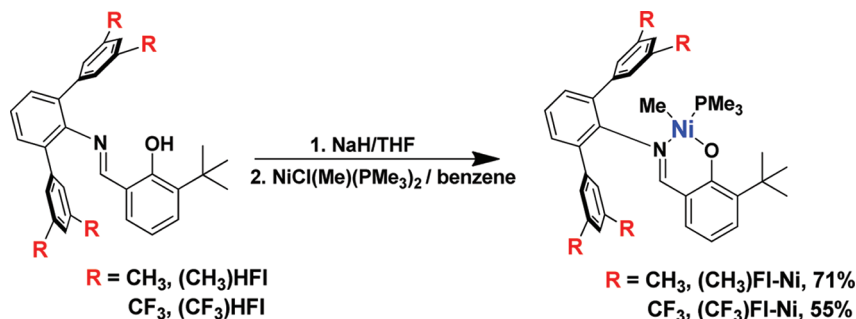
$(CH_3)FI\text{-Ni}$  and  $(CF_3)FI\text{-Ni}$  were confirmed in detail by NMR spectroscopy, elemental analysis, and X-ray diffraction. To further probe the effects that the electron-withdrawing ligand  $CF_3$  substituents might have on these catalysts, a complex was targeted with the  $CF_3$  substituent in closer proximity to the Ni center,  $(C=NCF_3)FI\text{-Ni}$ . Attempted condensation of 2,6-diisopropylaniline with  $\omega,\omega,\omega$ -trifluoro-2-hydroxy-3-*tert*-butylacetophenone

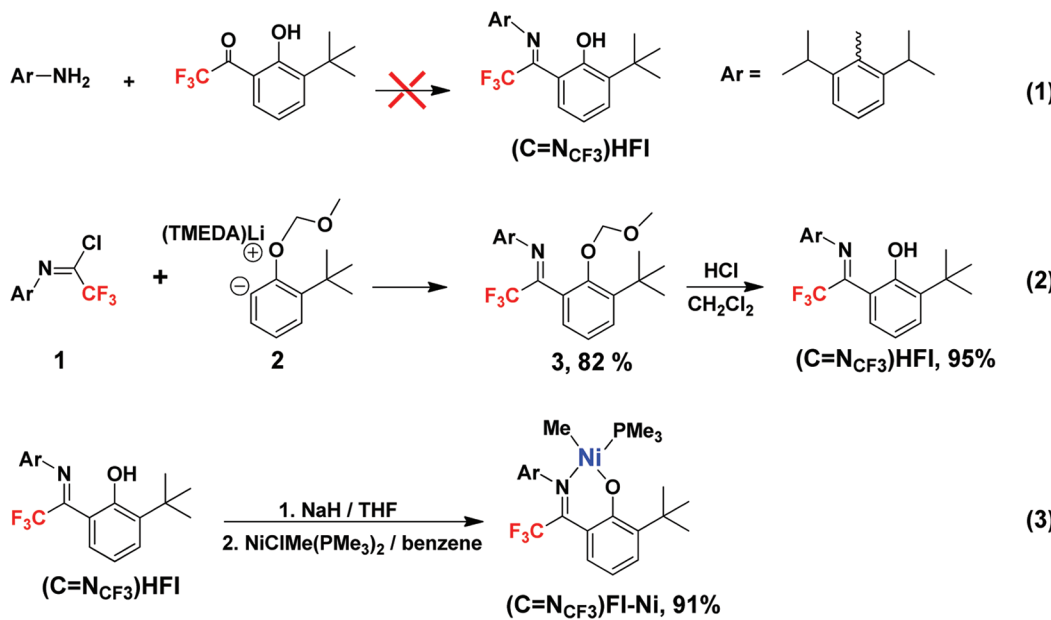
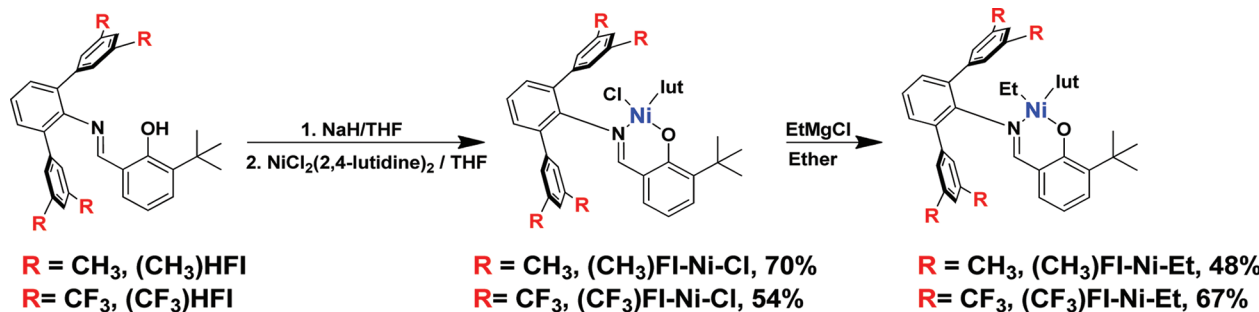
under a variety of conditions either does not yield the ligand  $(C=NCF_3)HFI$  or affords a mixture of products with low yields of  $(C=NCF_3)HFI$  which cannot be readily isolated (Scheme 2, eq 1). Thus, a new approach was developed that affords the ligand  $(C=NCF_3)HFI$  in very high yield (Scheme 2, eq 2). Reaction of *N*-(2,6-diisopropylphenyl)-2,2,2-trifluoroacetimidoyl chloride (1) with 2-methoxymethoxy-3-*tert*-butylphenyl lithium·TMEDA (2) affords the MOM-protected ligand precursor 3. MOM deprotection with HCl in  $CH_2Cl_2$  then affords the ligand  $(C=NCF_3)HFI$  in 95% yield.  $(C=NCF_3)HFI$  was next treated with NaH to produce the corresponding sodium salt, which was used for an *in situ* reaction with *trans*- $NiClMe(PMe_3)_2$  to afford the complex  $(C=NCF_3)FI\text{-Ni}$  in 91% yield (Scheme 2, eq 3).

To model a growing polyethylene chain, complexes  $(CF_3)FI\text{-Ni-Et}$  and  $(CH_3)FI\text{-Ni-Et}$  were synthesized from the Ni-Cl precursor complexes  $(CF_3)FI\text{-Ni-Cl}$  or  $(CH_3)FI\text{-Ni-Cl}$  by reacting the ligand sodium salts with  $NiCl_2(2,4\text{-lutidine})_2$  in THF (Scheme 3); complexes  $(CF_3)FI\text{-Ni-Et}$  and  $(CH_3)FI\text{-Ni-Et}$  were then prepared by alkylation with EtMgCl in diethyl ether (Scheme 3). Complexes  $(CF_3)FI\text{-Ni-Et}$  and  $(CH_3)FI\text{-Ni-Et}$  were isolated as red microcrystalline air-sensitive powders that are stable for weeks at room temperature without significant decomposition. The ligand 2,4-lutidine was chosen on the basis of literature precedent, showing that lutidine sufficiently stabilizes Ni-alkyl complexes with  $\beta\text{-H's}$ .<sup>26,40</sup>

**Molecular Structure of  $(CF_3)FI\text{-Ni}$ .** Single crystals of the precatalyst  $(CF_3)FI\text{-Ni}$  were grown by slowly cooling an *n*-pentane/toluene solution under  $N_2$ .  $(CF_3)FI\text{-Ni}$  crystallizes in triclinic space group  $P\bar{1}$  with two molecules in the asymmetric unit. Two *intermolecular* Ar-H…F–C hydrogen bonds<sup>41</sup> are evident, with distances ranging from 2.52 to 2.66  $\text{\AA}$ .<sup>42</sup>  $(CF_3)FI\text{-Ni}$  displays a distorted-square-planar geometry around the Ni atom with P1 and C1 displaced +0.363(3) and -0.368(2)  $\text{\AA}$  from the Ni/O1/N1 mean plane, respectively (Figure 2). Despite the distorted-square-planar solid-state geometry,  $(CF_3)FI\text{-Ni}$  and all other catalysts reported here exhibit diamagnetic NMR chemical shifts in solution. The Ni- $PM_3$  substituent is positioned trans to the imine functionality; this solid-state geometry was confirmed in solution by 1D  $^1H$  NOE experiments. A 50% displacement ellipsoid plot of  $(CF_3)FI\text{-Ni}$  and a space-filling model showing the nonbonded interactions in  $(CF_3)FI\text{-Ni}$  are shown in Figure 2. Interestingly, one terphenyl ring exhibits an intramolecular Ni…arene centroid distance of 3.864  $\text{\AA}$ . This Ni…centroid distance is much longer than in typical Ni–arene complexes, where average crystallographic distances from the 11 current structures in the Cambridge Structural Database are much shorter (1.65(4)  $\text{\AA}$ ).<sup>43</sup> Similar

### Scheme 1. Synthesis of Catalysts $(CH_3)FI\text{-Ni}$ and $(CF_3)FI\text{-Ni}$



Scheme 2. Synthesis of Catalyst  $(C=N_{CF_3})FI-Ni$ Scheme 3. Synthesis of Model Compounds  $(CH_3)FI-Ni-Et$  and  $(CF_3)FI-Ni-Et$ 

intramolecular Ni···arene contacts are also seen in related terphenyl phenoxyimine nickel complexes<sup>11b,e</sup> and in the solid-state structure of  $(CH_3)FI-Ni$ . No evidence of significant Ni···F interactions is observed in  $(CF_3)FI-Ni$ , with the closest Ni···F distance being 4.299(2) Å (Ni···F6); the sum of the Ni and F van der Waals radii is 3.31 Å.<sup>44</sup>

**Molecular Structure of  $(CH_3)FI-Ni$ .** X-ray-quality crystals of the precatalyst  $(CH_3)FI-Ni$  were grown by slowly cooling an *n*-hexane/toluene solution under  $N_2$ .  $(CH_3)FI-Ni$  crystallizes in the triclinic space group  $P\bar{1}$ . The coordination environment around Ni is similar to the structure of  $(CF_3)FI-Ni$ , with the  $PM_3$  ligand trans to the imine functionality (Figure 3). A distorted-square-planar geometry around the Ni is observed with atoms P1 and C1 displaced +0.403(3) and -0.392(4) Å from the Ni/O1/N1 mean plane, respectively. Interestingly, despite the different electronic characteristics of  $(CF_3)FI-Ni$  and  $(CH_3)FI-Ni$ , the Ni–phenoxyimine ligand bond distances in these complexes are crystallographically identical (*vide infra*).  $(CH_3)FI-Ni$  exhibits a shorter Ni–Me bond distance relative to  $(CF_3)FI-Ni$  (1.937(3) and 1.953(2) Å, respectively). A displacement ellipsoid plot of  $(CH_3)FI-Ni$  is shown in Figure 3.  $(CH_3)FI-Ni$  exhibits an intramolecular Ni···arene centroid distance of 3.695 Å.

**Molecular Structure of  $(CF_3)FI-Ni-Et$ .** Single crystals of  $(CF_3)FI-Ni-Et$  were grown by slow evaporation of an *n*-hexane solution under  $N_2$ . A 50% displacement ellipsoid plot of the 70% conformer of  $(CF_3)FI-Ni-Et$  is shown in Figure 4.

$(CF_3)FI-Ni-Et$  crystallizes in space group  $P2_1/c$  with four molecules in the asymmetric unit and displays a distorted-square-planar geometry around the Ni atom with N1 and C1 displaced +0.120(2) and -0.326(3) Å from the Ni/O1/N1 mean plane. The spatial configuration around the Ni in  $(CF_3)FI-Ni-Et$  indicates that the Ni–lutidine substituent is positioned trans to the imine functionality; that this solid-state geometry persists in solution is confirmed by 1D  $^1H$  NOE experiments. The 2,4-lutidine plane is oriented nearly perpendicular to the Ni/C1/O1 plane, with a C1/Ni/N1/C7 torsion angle of 87.4°. In comparison to the Ni–ligand bond distances in  $(CH_3)FI-Ni$  and  $(CF_3)FI-Ni$ , the Ni–N2 and Ni–O bond distances are significantly shorter in  $(CF_3)FI-Ni-Et$  (e.g., Ni–N<sub>imine</sub> = 1.936(2) and 1.893(1) Å for  $(CF_3)FI-Ni$  and  $(CF_3)FI-Ni-Et$ , respectively). The Ni–N(lutidine) distance is not unexpectedly shorter than the Ni– $PM_3$  contacts in  $(CH_3)FI-Ni$  and  $(CF_3)FI-Ni$ . Relative to the  $PM_3$ -coordinated  $(CH_3)FI-Ni$  and  $(CF_3)FI-Ni$ , the shorter Ni–N and Ni–O bond distances in 2,4-lutidine-coordinated  $(CF_3)FI-Ni-Et$  likely reflect the more electron-deficient metal center due to the stronger  $\pi$ -acid characteristics of 2,4-lutidine.<sup>45</sup> A 70%/30% conformational disorder is found about the Ni–Et axis, and this was modeled appropriately in the Ni–Et conformation as well as for F atoms F10, F11, and F12 (80%/20%).<sup>46</sup> The closer F···H distance in the 70% conformer is consistent with an energetically more favorable orientation. The derived

(C)F···H(C) distance in this precatalyst is greater than the sum of the CH<sub>3</sub> and F van der Waals radii (2.57 Å).<sup>44</sup> Nevertheless, molecular modeling<sup>34</sup> reveals that, during polymerization, (C<sub>β</sub>)H<sub>β</sub>···F(C) distances can be as small as ~2.61 Å (vide infra). No significant Ni···F interactions are observed in (CF<sub>3</sub>)FI-Ni-Et, with the closest Ni···F contact being 4.113(2) Å, longer than the sum of Ni and F van der Waals radii (3.31 Å).<sup>44</sup> Similar to the case for (CF<sub>3</sub>)FI-Ni, the crystal packing of (CF<sub>3</sub>)FI-Ni-Et features close intermolecular C–H···F hydrogen bond contacts with an H···F distance of 2.41 Å;<sup>42</sup> the sum of the H and F van der Waals radii is 2.57 Å.<sup>44</sup>

**Molecular Structure of (C=N<sub>CF<sub>3</sub></sub>)FI-Ni.** Single crystals of precatalyst (C=N<sub>CF<sub>3</sub></sub>)FI-Ni were grown by slowly cooling an *n*-pentane solution under N<sub>2</sub>. Complex (C=N<sub>CF<sub>3</sub></sub>)FI-Ni crystallizes in space group P2<sub>1</sub>/c. A 50% displacement ellipsoid plot of (C=N<sub>CF<sub>3</sub></sub>)FI-Ni is shown in Figure 5. The coordination environment of Ni is similar to that in the structures of (CH<sub>3</sub>)FI-Ni and (CF<sub>3</sub>)FI-Ni, with the Ni–PMe<sub>3</sub> ligand trans to the imine functionality. A distorted-square-planar geometry around the Ni is observed, with atoms P1 and C1 displaced +0.403(3) and -0.643(2) Å from the Ni/O1/N1 mean plane. Relative to (CH<sub>3</sub>)FI-Ni and (CF<sub>3</sub>)FI-Ni, (C=N<sub>CF<sub>3</sub></sub>)FI-Ni exhibits a significantly shorter Ni–O bond distance and a significantly longer Ni–N bond distance.

**Ethylene Polymerization Experiments.** (CH<sub>3</sub>)FI-Ni, (CF<sub>3</sub>)FI-Ni, and (C=N<sub>CF<sub>3</sub></sub>)FI-Ni are active ethylene polymerization/oligomerization catalysts in the presence of Ni(COD)<sub>2</sub> as a phosphine scavenger/cocatalyst. In the absence of cocatalyst, negligible polyethylene is produced by any of the complexes. Typical experiments were conducted with 5.0 μmol of catalyst in 50 mL of toluene under a continuous 8.0 atm ethylene pressure for 10.0 min using conditions minimizing mass transport and exotherm effects.<sup>8,e,g–j</sup> Relevant data are compiled in Table 1. The polymeric products were characterized by <sup>1</sup>H and <sup>13</sup>C NMR and gel permeation chromatography (GPC) using refractive index and viscometry detection. Polyethylene branch densities were assayed by <sup>1</sup>H NMR spectroscopy.<sup>30</sup> The type of branching observed in all the polyethylenes produced by the present catalysts is predominantly methyl, with a small percentage of longer chains ( $\geq C_6$ ).

At 25 °C, CF<sub>3</sub>-substituted (CF<sub>3</sub>)FI-Ni is ~6.5× more active than the CH<sub>3</sub>-substituted analogue (CH<sub>3</sub>)FI-Ni (250 vs 38 kg of polymer (mol of Ni)<sup>-1</sup> h<sup>-1</sup> atm<sup>-1</sup>, respectively), with the resulting polyethylene displaying dramatically greater M<sub>w</sub> (92 000 vs 1400 g mol<sup>-1</sup>, respectively), and far lower alkyl branch density (7 vs 88 branches/1000C, respectively). Figure 6 shows <sup>13</sup>C NMR spectra illustrating the substantially greater chain branching introduced in the polyethylenes produced by (CH<sub>3</sub>)FI-Ni vs those produced by (CF<sub>3</sub>)FI-Ni. In addition to

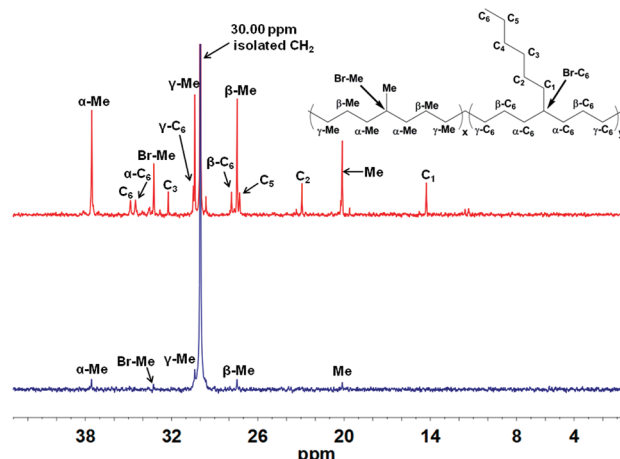


Figure 6. Stack plot showing <sup>13</sup>C{<sup>1</sup>H} NMR spectra (400 MHz, 120 °C, 1,1,2,2-tetrachloroethane-*d*<sub>6</sub>) of polyethylenes produced in room-temperature polymerizations under the same reaction conditions using catalysts (CH<sub>3</sub>)FI-Ni (top) and (CF<sub>3</sub>)FI-Ni (bottom).

increased M<sub>w</sub>'s and depressed branching, the ethylene polymerizations carried out at 50 °C reveal that the (CF<sub>3</sub>)FI-Ni catalyst has a thermal stability substantially greater than that derived from (CH<sub>3</sub>)FI-Ni, as judged by the marked fall in activity for (CH<sub>3</sub>)FI-Ni at 50 °C (Table 1).

The ethylene pressure dependence of the room-temperature ethylene polymerization activity of (CF<sub>3</sub>)FI-Ni was also investigated (Table 2, Figure 7). First-order dependence of the TOF on ethylene pressure is observed over an 8-fold pressure range, with product branch densities progressively falling with increasing ethylene pressure and molecular weights initially increasing and then saturating with increasing ethylene pressure. These data suggest competition between insertive propagation and chain transfer/chain walking via β-hydride elimination (vide infra). In the presence of Ni(COD)<sub>2</sub>, (C=N<sub>CF<sub>3</sub></sub>)FI-Ni is a modestly active ethylene oligomerization catalyst (7.9 kg of oligomer (mol of Ni)<sup>-1</sup> h<sup>-1</sup> atm<sup>-1</sup>; Table 1). The molecular weights of the oligomers produced by (C=N<sub>CF<sub>3</sub></sub>)FI-Ni were determined by GC-MS to range from C<sub>4</sub> to C<sub>26</sub> in an approximate Schulz–Flory distribution.<sup>42,47</sup> Oligomer end group analysis by <sup>1</sup>H NMR spectroscopy reveals predominantly internal olefinic groups (~90%) with a small percentage (~10%) of vinyl end groups.<sup>42</sup>

## DISCUSSION

**Propagation and Chain Transfer Pathways.** Ethylene polymerization experiments were conducted as a function of ethylene pressure using (CF<sub>3</sub>)FI-Ni to probe the operative chain transfer and propagation pathways in this system. Over

Table 1. Ethylene Polymerization Data for Fluorocarbon-Substituted and Fluorine-Free Catalysts<sup>a</sup>

entry	cat.	temp (°C)	polymer yield (g)	M <sub>w</sub> (10 <sup>3</sup> g mol <sup>-1</sup> ) <sup>d</sup>	PDI <sup>d</sup>	total Me/1000C <sup>e</sup>	activity <sup>f</sup>
1	(CH <sub>3</sub> )FI-Ni <sup>b</sup>	23	0.253	1.4	1.1	88	38
2	(CF <sub>3</sub> )FI-Ni <sup>b</sup>	23	1.661	92.0	3.0	7	250
3	(C=N <sub>CF<sub>3</sub></sub> )FI-Ni <sup>c</sup>	23	0.419	C4–C26			7.9
4	(CH <sub>3</sub> )FI-Ni <sup>b</sup>	50	0.047	0.95	1.5	109	7.1
5	(CF <sub>3</sub> )FI-Ni <sup>b</sup>	50	3.042	7.9	2.2	40	460

<sup>a</sup>Polymerizations carried out at 8.0 atm of ethylene pressure for 10.0 min using 2.0 equiv of Ni(COD)<sub>2</sub>. Polymerizations were performed in duplicate. <sup>b</sup>Polymerizations with 5 μmol of catalyst for 10 min in 50 mL of toluene. <sup>c</sup>Polymerizations with 10 μmol of catalyst for 40 min in 25 mL of toluene. <sup>d</sup>GPC vs polystyrene standards. <sup>e</sup><sup>1</sup>H NMR assay. <sup>f</sup>In units of kg of polymer (mol of Ni)<sup>-1</sup> h<sup>-1</sup> atm<sup>-1</sup>.

the ethylene pressures studied, polymerizations are approximately first-order in [ethylene], the polymer  $M_w$  initially increases then saturates with increasing [ethylene], and polyethylene branch densities decrease with increasing [ethylene] (Table 2, Figure 7). These observations are in accord with

**Table 2. Ethylene Polymerization Data as a Function of Ethylene Pressure Utilizing  $(CF_3)_2FI-Ni^a$**

entry	pressure (atm)	TOF <sup>b</sup> ( $\times 10^3$ h <sup>-1</sup> )	polymer yield (g)	$M_w^c$ ( $\times 10^3$ g mol <sup>-1</sup> )	PDI	total Me/1000C <sup>c</sup>
1	1.0	4.6	0.107	40	2.6	27
2	3.0	24	0.572	72	2.6	13
3	5.0	53	1.247	81	3.5	11
4	8.0	70	1.632	92	3.0	7

<sup>a</sup>Polymerizations carried out in 25 mL of toluene at 8.0 atm ethylene pressure at 50 °C with 2.0 equiv of  $Ni(COD)_2$ . Polymerizations were carried out with 5.0  $\mu$ mol of catalyst. <sup>b</sup>TOF = mol of  $C_2H_4$  (mol of Ni)<sup>-1</sup> h<sup>-1</sup>. <sup>c</sup>By <sup>1</sup>H NMR assay.

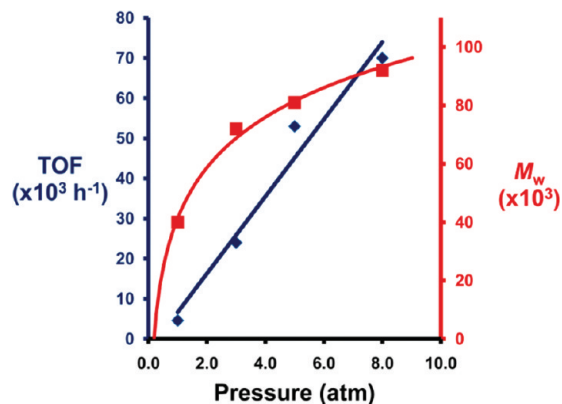
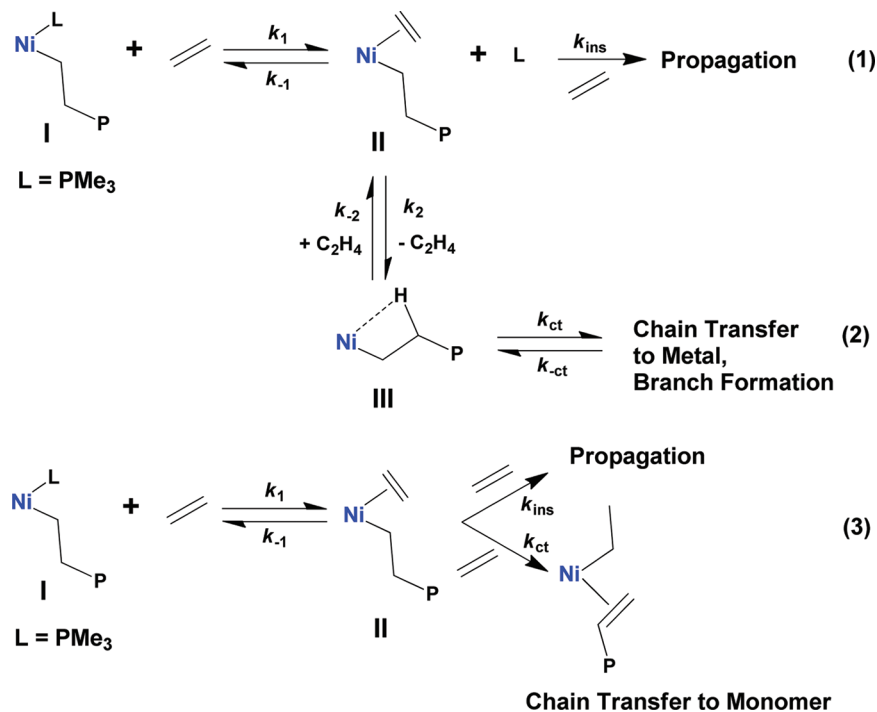


**Figure 7.** Ethylene pressure dependence of  $(CF_3)_2FI-Ni$ -mediated ethylene polymerization.

a scenario as in Scheme 4 (eq 1), where increasing  $M_w$  with increasing [ethylene] implicates chain transfer to the metal ( $\beta$ -hydride elimination) as the predominant chain transfer pathway,<sup>48</sup> rather than chain transfer to monomer, which should ideally yield a constant  $M_w$  with increasing [ethylene] (Scheme 4 (eq 3)) because the propagation/chain transfer branch ratio is independent of [ethylene].<sup>49</sup> Depending on the details of the relative rate constants, TOF vs [ethylene] plots may saturate at very high [ethylene], obeying essentially Michaelis–Menten kinetics, as observed for related neutrally charged Ni(II) catalysts at ethylene pressures >30 bar.<sup>11b,40</sup> This behavior and parallel saturation in product  $M_w$  may also reflect high- $M_w$  polyethylene precipitation, which is observed at elevated ethylene pressures (>5.0 atm) and would inhibit monomer diffusion to the catalyst. Additionally, at higher ethylene pressures, polyethylene branching is expected to fall due to ethylene interception of intermediate agostic species such as III, thereby suppressing chain transfer and favoring propagation via species such as II (Scheme 4, eqs 1 and 2).<sup>4b,50</sup>

As noted above, installation of  $CF_3$  substituents in  $(CF_3)_2FI-Ni$  results in  $\sim 6.5\times$  greater activity than for the  $CH_3$ -substituted analogue ( $CH_3)_2FI-Ni$  (250 vs 38 kg of polymer (mol of Ni)<sup>-1</sup> h<sup>-1</sup> atm<sup>-1</sup>, respectively), with the resulting polyethylene displaying dramatically greater  $M_w$  (92 000 vs 1400 g mol<sup>-1</sup>, respectively), and far lower alkyl branch densities (7 vs 88 branches/1000C, respectively). Since chain-walking processes are typically accompanied by slow ethylene insertion into secondary Ni–alkyl linkages,<sup>6f</sup> suppression of  $\beta$ -H elimination/chain walking in  $(CF_3)_2FI-Ni$  would reasonably enhance activity and  $M_w$  vs  $(CH_3)_2FI-Ni$ , which undergoes significantly greater competing chain walking. In addition to the increased  $M_w$ 's and depressed branching, 50 °C ethylene polymerization experiments reveal that  $CF_3$ -substituted  $(CF_3)_2FI-Ni$  displays substantially greater thermal stability than  $CH_3$ -substituted  $(CH_3)_2FI-Ni$ , judging from the marked fall in activity for  $(CH_3)_2FI-Ni$  at 50 °C (Table 1). The deactivation

**Scheme 4. Chain Transfer Scenarios and  $M_w$  Dependence on [ethylene]**



pathways for these types of catalysts are known to be triggered by  $\beta$ -H elimination to form unstable Ni hydrides.<sup>51</sup> In the present case, ligand trifluoromethylation kinetically retards  $\beta$ -H elimination, leading to enhanced thermal stability. To further investigate the scope of  $\text{CF}_3$  substitution effects on the present catalytic behavior, the complex ( $\text{C}=\text{N}_{\text{CF}_3}$ )FI-Ni was designed with a  $\text{CF}_3$  group located in closer proximity to the Ni center. In direct contrast to the effects observed in the relative properties of ( $\text{CH}_3$ )FI-Ni and ( $\text{CF}_3$ )FI-Ni, ( $\text{C}=\text{N}_{\text{CF}_3}$ )FI-Ni only catalyzes ethylene oligomerization with low activity.<sup>52</sup> If simple inductive effects were responsible for the substantial  $M_w$  and activity increases in ( $\text{CF}_3$ )FI-Ni, these effects might reasonably be observed or enhanced in ( $\text{C}=\text{N}_{\text{CF}_3}$ )FI-Ni.

Considering the dramatic effects that the introduction of electron-withdrawing  $\text{CF}_3$  groups have on the ethylene polymerization properties of the present catalysts, the possible contribution of electronic effects was investigated. Non-negligible distal  $\text{CF}_3$  ligand substituent effects, among other effects, on group 10 mediated polymerizations and the resulting polymer structures were noted previously and ascribed to electronic/inductive effects.<sup>3k,11b,e,51</sup> While such effects may be operative here, the NMR spectral parameters of the present complexes do not evidence clear substituent-related chemical shift patterns (Table 3). Thus, NMR spectra exhibit no

**Table 3. Electronic Structure Diagnostic NMR Spectral Data (ppm) in Complexes ( $\text{CH}_3$ )FI-Ni, ( $\text{CF}_3$ )FI-Ni, and ( $\text{C}=\text{N}_{\text{CF}_3}$ )FI-Ni**

complex	$^1\text{H}$ , $\text{Ni}-\text{CH}_3, \delta$	$^{13}\text{C}$ , $\text{Ni}-\text{CH}_3, \delta$	$^{31}\text{P}$ , $\text{PMe}_3, \delta$	$^{13}\text{C}$ , $\text{C}=\text{N}, \delta$
( $\text{CH}_3$ )FI-Ni	-0.98	-13.68	-13.8	168.45
( $\text{CF}_3$ )FI-Ni	-1.33	-13.48	-12.6	168.20
( $\text{C}=\text{N}_{\text{CF}_3}$ )FI-Ni	-1.41	-11.5	-14.8	169.0

significant differences in the chemical shifts of the  $\text{Ni}-\text{CH}_3$  or the imine C signals in ( $\text{CH}_3$ )FI-Ni and ( $\text{CF}_3$ )FI-Ni that might be expected for through-bond electronic communication. Additionally, there is no discernible pattern in the bound  $\text{PMe}_3$   $^{31}\text{P}$  NMR chemical shifts. In the  $^1\text{H}$  NMR, the  $\text{Ni}-\text{CH}_3$  signal exhibits an unexpected upfield shift as trifluoromethylation is introduced. While these observations do not rule out remote substituent inductive effects on the polymerization pathway, there is no NMR evidence to support this. Furthermore, analysis of the diffraction-derived metrical parameters in ( $\text{CH}_3$ )FI-Ni, ( $\text{CF}_3$ )FI-Ni, and ( $\text{C}=\text{N}_{\text{CF}_3}$ )FI-Ni reveals no systematic evidence of electronic effects at the Ni center in the precatalysts. Selected bond distances for complexes ( $\text{CH}_3$ )FI-Ni, ( $\text{CF}_3$ )FI-Ni, and ( $\text{C}=\text{N}_{\text{CF}_3}$ )FI-Ni are compared in Table 4. The  $\text{Ni}-\text{O}$  and  $\text{Ni}-\text{N}$

**Table 4. Electronic Structure Diagnostic Bond Distances in Complexes ( $\text{CH}_3$ )FI-Ni, ( $\text{CF}_3$ )FI-Ni, and ( $\text{C}=\text{N}_{\text{CF}_3}$ )FI-Ni**

complex	$\text{Ni}-\text{CH}_3, \text{\AA}$	$\text{Ni}-\text{O}, \text{\AA}$	$\text{Ni}-\text{N}, \text{\AA}$	$\text{Ni}-\text{P}, \text{\AA}$
( $\text{CH}_3$ )FI-Ni	1.937(3)	1.917(2)	1.937(2)	2.1420(9)
( $\text{CF}_3$ )FI-Ni	1.953(2)	1.914(1)	1.936(2)	2.1496(6)
( $\text{C}=\text{N}_{\text{CF}_3}$ )FI-Ni	1.931(2)	1.900(1)	1.968(1)	2.1353(5)

bond distances are very similar in complexes ( $\text{CH}_3$ )FI-Ni and ( $\text{CH}_3$ )FI-Ni and ( $\text{C}=\text{N}_{\text{CF}_3}$ )FI-Ni also exhibit very similar  $\text{Ni}-\text{C}$  bond distances. Although the  $\text{Ni}-\text{CH}_3$  bond distance

in ( $\text{CF}_3$ )FI-Ni is significantly longer than the corresponding bond distances in ( $\text{CH}_3$ )FI-Ni and ( $\text{C}=\text{N}_{\text{CF}_3}$ )FI-Ni, there is no obvious trend in the  $\text{Ni}-\text{CH}_3$  bond lengths to support major inductive effects. It is also unlikely that steric effects alone are responsible for the marked polymerization differences between ( $\text{CH}_3$ )FI-Ni and ( $\text{CF}_3$ )FI-Ni, since the van der Waals radii of F and H are similar (1.47 and 1.10 Å, respectively).<sup>44</sup>

**C–H···F–C Interactions.** Considering the lack of evidence for  $\text{CF}_3$ -derived inductive effects and the large Ni–terphenyl substituent distances seen in the structural data, the possibility that weak C–F···H–C interactions<sup>16,17,41</sup> may disfavor chain transfer in ( $\text{CF}_3$ )FI-Ni by destabilizing the syn-periplanar conformation generally thought to facilitate  $\beta$ -H elimination<sup>53</sup> (e.g., Scheme 5) is considered as a reasonable alternative. For catalyst ( $\text{CH}_3$ )FI-Ni, all other factors being equal, the absence of such interactions would favor the correct conformation for elimination. The pathway depicted in Scheme 5 is consistent with observations (vide supra) that the predominant chain transfer pathway in these catalysts is  $\beta$ -H elimination (chain transfer to metal). To probe whether non-negligible C–F···H $_{\beta}$ –C $_{\beta}$  interactions might be operative in ( $\text{CF}_3$ )FI-Ni catalysis, the model ethyl complex ( $\text{CF}_3$ )FI-Ni-Et was synthesized from the Ni–Cl precursor ( $\text{CF}_3$ )FI-Ni-Cl (Scheme 3). ( $\text{CF}_3$ )FI-Ni-Et was characterized by NMR, elemental analysis, and X-ray diffraction (Figure 4).<sup>42</sup> The closest C–F···H–C(2) contact in the solid state (i.e., ground state) is 3.69 Å, longer than the sum of the H and F van der Waals radii (2.57 Å).<sup>44</sup> To probe the presence of such interactions in solution, 2D  $^{19}\text{F}$ – $^1\text{H}$  HOESY NMR<sup>54</sup> and 2D  $^1\text{H}$ – $^1\text{H}$  NOESY NMR experiments were carried out on ( $\text{CF}_3$ )FI-Ni-Et (Figure 8) and ( $\text{CH}_3$ )FI-Ni-Et (Figure S5 of the Supporting Information), respectively. In the  $^{19}\text{F}$ – $^1\text{H}$  HOESY NMR spectrum of ( $\text{CF}_3$ )FI-Ni-Et, two  $^{19}\text{F}$  signals corresponding to  $\text{CF}_3$  groups on each ring are observed at 25 °C, likely due to hindered rotation around the N–aryl bond, with free rotation about the aryl C–C bonds. In addition to the strong intra-ring  $^{19}\text{F}$ ··· $^1\text{H}$  dipolar contacts between the  $\text{CF}_3$  groups and *ortho* and *para* protons (Figure 8, bottom), several  $^{19}\text{F}$ ··· $^1\text{H}$  NOEs are observed (Figure 8, middle and top): CF<sub>3</sub>(A) interacts with the *o*-methyl of the 2,4-lutidine ligand (medium), CF<sub>3</sub>(B) with H14 of the 2,4-lutidine ligand (medium-weak), both CF<sub>3</sub>(A) and CF<sub>3</sub>(B) with the *tert*-butyl moiety (medium-weak), and both CF<sub>3</sub>(A) and CF<sub>3</sub>(B) with the methyl group of the  $\text{NiCH}_2\text{CH}_3$  moiety. The fact that CF<sub>3</sub>(A) and CF<sub>3</sub>(B) show selective interactions with the *o*-methyl and H14 of the 2,4-lutidine ligand, respectively, indicates that rotation of the lutidine about the Ni–N bond is slow. However, this motion is not fully frozen, since exchange cross-peaks are observed between H8/H9 and H11/H12 and between H10 and H13 in the  $^1\text{H}$  NOESY NMR spectrum recorded in the same solvent at the same temperature. In contrast, the methyl of the  $\text{NiCH}_2\text{CH}_3$  moiety exhibits comparable  $^{19}\text{F}$ ··· $^1\text{H}$  NOEs with both CF<sub>3</sub>(A) and CF<sub>3</sub>(B) and similar  $^1\text{H}$ ··· $^1\text{H}$  NOEs with both *o*-methyl and H14 hydrogen atoms of the lutidine ligand. This indicates that the energy barrier associated with rotation of the ethyl group around the Ni–C bond is small. In the  $^1\text{H}$ – $^1\text{H}$  NOESY NMR spectrum of ( $\text{CH}_3$ )FI-Ni-Et, observed NOE interactions are similar to those of ( $\text{CF}_3$ )FI-Ni-Et, suggesting the average 3D structures of the two complexes in solution are similar.

The  $^1\text{H}$  NMR chemical shifts in ( $\text{CF}_3$ )FI-Ni-Et and ( $\text{CH}_3$ )FI-Ni-Et (with the exception of those belonging to the

**Scheme 5.** Newman Projections Illustrating How Significant (ligand)F $\cdots$ H(alkyl-Ni) Interactions Would Disfavor the Syn-Periplanar Conformation for  $\beta$ -H Elimination

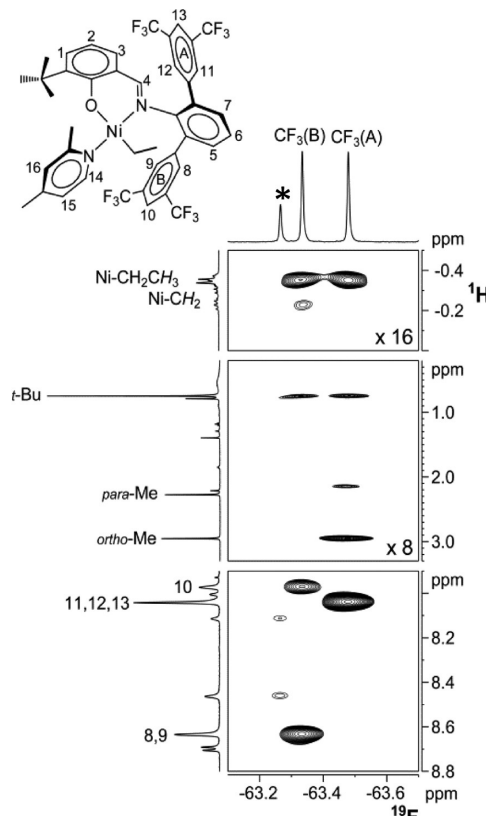
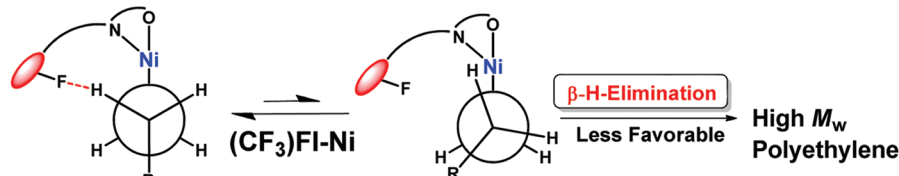
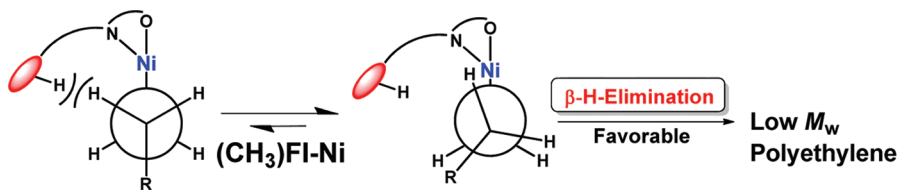
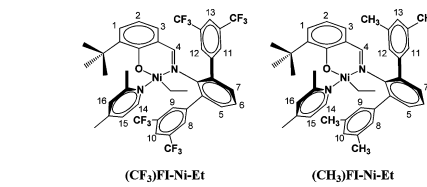


**Figure 8.** Three sections of the  $^{19}\text{F}$ – $^1\text{H}$  HOESY NMR spectrum ( $\text{CD}_2\text{Cl}_2$ , 298 K) showing  $^{19}\text{F}\cdots{}^1\text{H}$  dipolar interactions in the complex  $(\text{CF}_3)\text{FI-Ni-Et}$ . The asterisk indicates decomposition product.

terphenyl moiety) are tabulated in Figure 9, and the  $\Delta\delta$  values are graphically compared in Figure 10. The  $\text{CH}_3\text{CH}_2$  nuclei (“CH” in the table) are diastereotopic in both complexes and appear as complex multiplets (see Figures S6 and S9 of the Supporting Information for 2D  $^1\text{H}$ – $^{13}\text{C}$  HSQC NMR spectra of  $(\text{CH}_3)\text{FI-Ni-Et}$  and  $(\text{CF}_3)\text{FI-Ni-Et}$ , respectively). Note that simulation of these second-order spectra (AA'X<sub>3</sub> for  $(\text{CH}_3)\text{FI-Ni-Et}$  and ABM<sub>3</sub> for  $(\text{CF}_3)\text{FI-Ni-Et}$ , in which X<sub>3</sub> and M<sub>3</sub> represent the three H nuclei of the CH<sub>3</sub> group) indicates that it is not necessary to include scalar coupling with the F nuclei to reproduce the experimental multiplets (see Figures S3 and S7



Numbering	$\delta(\text{CH}_3)\text{FI-Ni-Et}$	$\delta(\text{CF}_3)\text{FI-Ni-Et}$	$\Delta\delta$
1	7.00	7.035	-0.035
2	6.160	6.191	-0.031
3	6.631	6.613	0.018
4	7.580	7.584	-0.003
t-Bu	0.780	0.727	0.053
14	8.650	8.684	-0.034
15	6.785	6.842	-0.057
16	6.856	6.874	-0.018
<i>o</i> -Me	3.109	2.947	0.162
<i>p</i> -Me	2.235	2.246	-0.011
CH(Et)	-0.204	-0.247	0.043
CH(Et)	-0.217	-0.318	0.101
CH <sub>3</sub> (Et)	-0.379	-0.373	-0.006

**Figure 9.**  $^1\text{H}$  NMR chemical shifts ( $\delta$ ) of model compounds  $(\text{CF}_3)\text{FI-Ni-Et}$  and  $(\text{CH}_3)\text{FI-Ni-Et}$ .

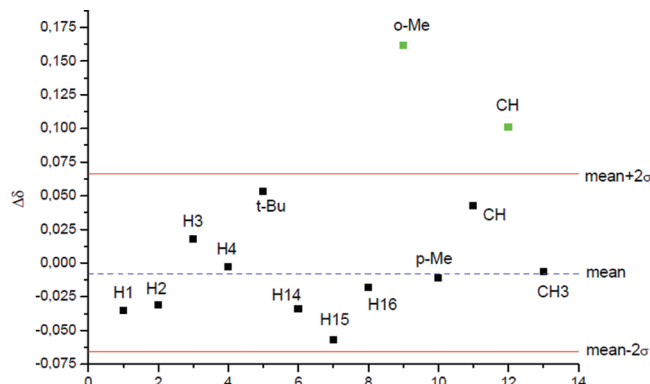


**Figure 10.** Comparison of  $^1\text{H}$  NMR chemical shifts in  $(\text{CF}_3)\text{FI-Ni-Et}$  and  $(\text{CH}_3)\text{FI-Ni-Et}$ .

of the Supporting Information), due to the fluxional nature of  $(\text{CF}_3)\text{FI-Ni-Et}$  in solution. In addition, the methylene  $^{13}\text{C}$  and methyl  $^{13}\text{C}$  resonances appear as singlets in the  $^{13}\text{C}\{^1\text{H}\}$  NMR spectrum (see Figure S8 of the Supporting Information), also confirming that is not necessary to include scalar coupling

Chart 5

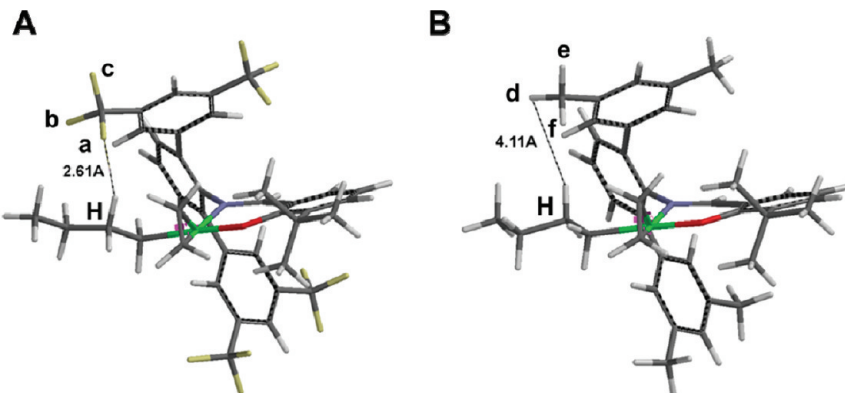
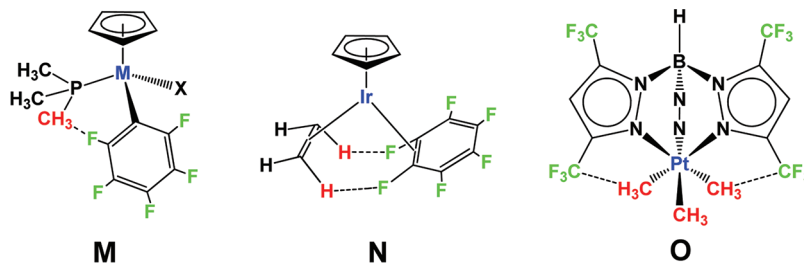


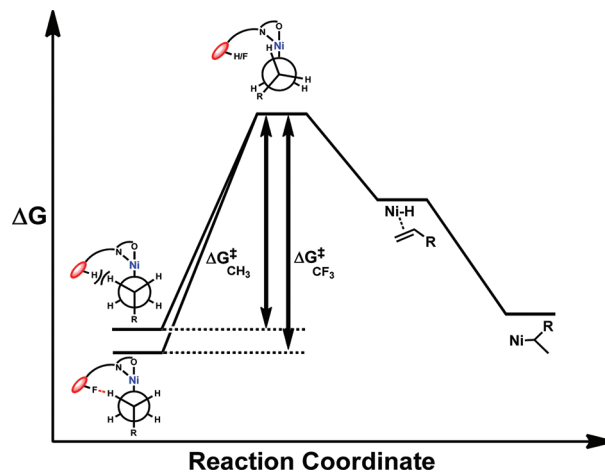
**Figure 11.** Spartan PM3/HF ab initio minimization of the polymerization-active catalysts derived from  $(CF_3)FI\text{-Ni}$  (A,  $C\text{-}F\cdots H_\beta\text{-}C_\beta = 2.61 \text{ \AA}$ ) and  $(CH_3)FI\text{-Ni}$  (B,  $C\text{-}H\cdots H_\beta\text{-}C_\beta = 4.11 \text{ \AA}$ ) with an *n*-butyl group modeling the polyethylene chain. Selected distances ( $\text{\AA}$ ) between F/H and  $H_\beta\text{-}C_\beta$ :  $H\text{-}a = 2.61$ ,  $H\text{-}b = 3.11 \text{ \AA}$ , and  $H\text{-}c = 3.68$  in  $(CF_3)FI\text{-Ni}$ ;  $H\text{-}d = 4.11$ ,  $H\text{-}e = 5.10$ , and  $H\text{-}f = 4.31$  in  $(CH_3)FI\text{-Ni}$ .

between the F and H nuclei. In this regard, non-negligible through-space  $^1\text{H}\cdots ^{19}\text{F}$  and  $^{13}\text{C}\cdots ^{19}\text{F}$  scalar coupling is frequently observed in molecules with rigid structures that impose short H...F contacts, such as  $(\eta^5\text{-C}_5\text{H}_5)\text{M}(\text{PMe}_3)\text{-}(C_6\text{F}_5)\text{X}$  ( $\text{M} = \text{Rh}, \text{Ir}$ ;  $\text{X} = \text{F}, \text{Cl}, \text{Br}$ ; **M**, Chart 5),<sup>55</sup>  $(\eta^5\text{-C}_5\text{H}_5)\text{Ir}(\text{C}_2\text{H}_4)(n^2\text{-C}_6\text{F}_6)$  (**N**, Chart 5),<sup>56</sup> and  $\text{Tp}^{(CF_3)_2}\text{PtMe}_3$  (**O**, Chart 5).

From Figures 9 and 10 it is evident that  $\Delta\delta$  values are much greater for some resonances than for others. In particular, the *o*-Me and one of the two  $\text{CH}_3\text{CH}_2-$  resonances are significantly more shielded in  $(CF_3)FI\text{-Ni-Et}$ . The mean  $\Delta\delta$  calculated using all  $\delta$  data except those of *o*-Me and one of the two  $\text{CH}_3\text{CH}_2-$  resonances (green in Figure 10) is  $-0.008 \text{ ppm}$  with a standard deviation of  $0.033 \text{ ppm}$ . The  $\Delta\delta$  values for *o*-Me and one of the two  $\text{CH}_3\text{CH}_2-$  resonances are more than 2 standard deviations away from the mean. This effect may be due to the close proximity of these groups to the electronic clouds of the F atoms, indicating a through-space dipolar interaction.<sup>58</sup> Inductive effects through the ligand scaffold are unlikely to be responsible for the large *o*-Me and  $\text{CH}_2$   $\Delta\delta$  values because (1) one of the two diastereotopic  $\text{CH}_2$  resonances is more affected than the other and (2) the *o*-Me H nuclei have a much greater  $\Delta\delta$  value than  $\text{H}_4$ , which is much closer (through bond) to the terphenyl substituents.

An estimation of relevant average internuclear H...F distances is obtained from quantitative analysis of the 2D  $^{19}\text{F}\text{-}^1\text{H}$  HOESY data. With the average  $\text{H10/CF}_3$ (B) internuclear distance ( $3 \text{ \AA}$ ) as a reference distance,<sup>59</sup> the following *average distances* can be calculated from the relative cross-peak integrals, taking into account the number of equivalent nuclei:<sup>60</sup>  $\langle r \rangle_{\text{NiCH}_2\text{CH}_3\text{-CF}_3(\text{A})} = 5.2 \text{ \AA}$ ;  $\langle r \rangle_{\text{NiCH}_2\text{CH}_3\text{-CF}_3(\text{B})} = 5.3 \text{ \AA}$ ;  $\langle r \rangle_{\text{o-methyl-}CF_3(\text{A})} = 4.1 \text{ \AA}$ . Note that these distances are

**Scheme 6. Qualitative Free Energy Profile Showing How (ligand)F...H(alkyl-Ni) Interactions Favor/Disfavor the Syn-Periplanar Conformational Pathway for  $\beta$ -H Elimination**



average F...H distances in  $(CF_3)FI\text{-Ni-Et}$  and do not represent a measure of the shortest possible F...H distance. No significant  $CF_3$  interactions involving the  $\text{NiCH}_2\text{CH}_3$   $\alpha$ -hydrogen atoms are observed in the 2D  $^{19}\text{F}\text{-}^1\text{H}$  HOESY experiments, and it is unlikely on the basis of the diffraction data that there are significant  $CF_3\cdots\text{Ni}$  interactions (Chart 1, C; Figure 1). Further evidence supporting a F...H $_\beta$  rather than a F...Ni interaction is the far higher polymerization activity of  $(CF_3)FI\text{-Ni}$  vs that of  $(CH_3)FI\text{-Ni}$ . In previous reports, such F...M interactions (Chart 1, structure D) are accompanied by depressed polymerization activity, likely reflecting significant active site steric/coordinative electronic constraints.<sup>10</sup>

Molecular modeling<sup>34</sup> performed on the assumed polymerization-active catalytic species derived from  $(CF_3)_2FI\text{-Ni}$  with an *n*-butyl group to simulate the propagating polyethylene chain reveals that  $C_\beta\text{-H}_\beta\cdots F(C)$  distances in such species can be as small as  $\sim 2.61 \text{ \AA}$  (Figure 11A).<sup>42</sup> The exact same calculation performed on  $(CH_3)_2FI\text{-Ni}$  yields a much longer H $\cdots$ H distance of  $4.11 \text{ \AA}$  (Figure 11B).

Many experimental and theoretical studies have described C $\text{-F}\cdots\text{H-C}$  interactions as a type of hydrogen bond.<sup>41,61</sup> A theoretical study of the hydrogen bonding in  $CH_3F\cdots H_4C$  computed an interaction energy of  $-1.62 \text{ kJ/mol}$  in the gas phase.<sup>41c</sup> C $\text{-F}\cdots\text{H-C}$  hydrogen bonding has been shown to stabilize the solid-state structures of fluorobenzenes with experimental F $\cdots$ H distances in the range  $2.41\text{--}2.86 \text{ \AA}$ .<sup>62</sup> Also, rotational spectroscopy performed on  $CH_3F\cdots HCF_3$  provided detailed information on the chemical features of the C $\text{-F}\cdots\text{H-C}$  hydrogen bond and the internal dynamics of the pair.<sup>61b</sup> Furthermore, as exemplified by structures K and L above, C $\text{-H}\cdots\text{F-C}$  interactions have been proposed to influence enantioselectivity in reactions involving formyl groups, e.g. aldol condensation,<sup>23b $\text{--e}$</sup>  and to stabilize ammonium salts in olefin epoxidation catalysts.<sup>23a</sup> Additionally, as noted above, in the present crystal structures of  $(CF_3)_2FI\text{-Ni}$  and  $(CF_3)_2FI\text{-Ni-Et}$ , the solid-state packing is dominated by short intermolecular C $\text{-H}\cdots\text{F-C}$  hydrogen bonds with H $\cdots$ F distances of  $2.52$  and  $2.41 \text{ \AA}$ , respectively.

## CONCLUSIONS

Two phenoxyiminato Ni(II) catalysts where remote  $CF_3/CH_3$  substituents exert dramatically different effects on ethylene polymerization are reported. Remote  $CF_3$  substituents enhance activity, thermal stability, and product  $M_w$  and depress polyethylene branching vs the corresponding  $CH_3$ -substituted catalyst. Rather than invoking inductive effects, we propose that such  $CF_3$  substituents participate in C $\text{-F}\cdots\text{H-C}$  interactions involving the growing polyethylene chain, destabilizing the syn-periplanar conformation which favors  $\beta$ -hydride elimination (Scheme 5). Scheme 6 illustrates qualitatively how such a C $\text{-F}\cdots\text{H-C}$  interaction might disfavor chain transfer via  $\beta$ -H elimination.<sup>40,49a,b</sup> In the case of methyl-substituted  $(CH_3)_2FI\text{-Ni}$ , the absence of such interactions leads to a slightly more favorable  $\Delta G^\ddagger$  for  $\beta$ -H elimination. The suppression of  $\beta$ -H elimination also leads to significantly enhanced catalyst  $(CF_3)_2FI\text{-Ni}$  thermal stability. Heteronuclear 2D  $^{19}F_1^1H$  HOESY NMR spectroscopy and molecular modeling of a Ni- $CH_2CH_2CH_2CH_3$  complex provide evidence that the propagating polyethylene chain can be in close proximity to the remote ligand  $CF_3$  substituents, thereby disfavoring chain transfer. Additionally, the ethylene insertion behavior of  $(C=N_{CF_3})_2FI\text{-Ni}$ , where the electron-withdrawing  $CF_3$  moiety is in close proximity to the metal center, argues that dominant inductive effects in  $(CF_3)_2FI\text{-Ni}$  would alter the propagation and chain transfer kinetics in ways opposite to what is observed.

## ASSOCIATED CONTENT

### Supporting Information

Figures, tables, and CIF files giving catalyst and polymer characterization data and crystal data for  $(CH_3)_2HFI$ ,  $(CF_3)_2FI\text{-Ni}$ ,  $(CF_3)_2FI\text{-Ni-Et}$ , and  $(C=N_{CF_3})_2FI\text{-Ni}$ . This material is available free of charge via the Internet at <http://pubs.acs.org>.

## AUTHOR INFORMATION

### Corresponding Author

\*Tel (+1) 847 491 5658 (T.J.M.). Fax (+1) 847 491 2990 (T.J.M.). E-mail: m-delferro@northwestern.edu (M.D.); t-marks@northwestern.edu (T.J.M.).

### Notes

The authors declare no competing financial interest.

## ACKNOWLEDGMENTS

Financial support by the DOE (Grant 86ER13511) is gratefully acknowledged. We thank Dr. C. Weiss, Ms. J. McInnis, Mr. S. Wobser, and Dr. A. Spokoyny for helpful discussions.

## REFERENCES

- (1) For recent reviews of group 10 olefin polymerization catalysis, see: (a) Takeuchi, D. *Dalton Trans.* **2010**, *39*, 311–328. (b) Nakamura, A.; Ito, S.; Nozaki, K. *Chem. Rev.* **2009**, *109*, 5215–5244. (c) Chen, E. Y. X. *Chem. Rev.* **2009**, *109*, 5157–5214. (d) Domski, G. J.; Rose, J. M.; Coates, G. W.; Bolig, A. D.; Brookhart, M. *Prog. Polym. Sci.* **2007**, *32*, 30–92. (e) Zhang, J.; Wang, X.; Jin, G. X. *Coord. Chem. Rev.* **2006**, *250*, 95–109. (f) Durand, J.; Milani, B. *Coord. Chem. Rev.* **2006**, *250*, 542–560. (g) Gibson, V. C.; Spitzmesser, S. K. *Chem. Rev.* **2003**, *103*, 283–316. (h) Mecking, S. *Coord. Chem. Rev.* **2000**, *203*, 325–351. (i) Ittel, S. D.; Johnson, L. K.; Brookhart, M. *Chem. Rev.* **2000**, *100*, 1169–1204. (j) Boffa, L. S.; Novak, B. M. *Chem. Rev.* **2000**, *100*, 1479–1493. (k) Britovsek, G. J. P.; Gibson, V. C.; Wass, D. F. *Angew. Chem., Int. Ed.* **1999**, *38*, 428–447.
- (2) (a) Guironnet, D.; Friedberger, T.; Mecking, S. *Dalton Trans.* **2009**, *41*, 8929–8934. (b) Guironnet, D.; Goettker-Schnetmann, I.; Mecking, S. *Macromolecules* **2009**, *42*, 8157–8165. (c) Camacho, D. H.; Guan, Z. *Macromolecules* **2005**, *38*, 2544–2546. (d) Camacho, D. H.; Salo, E. V.; Ziller, J. W.; Guan, Z. *Angew. Chem., Int. Ed.* **2004**, *43*, 1821–1825. (e) Guan, Z. *Chem. Eur. J.* **2002**, *8*, 3086–3092. (f) Mecking, S. *Angew. Chem., Int. Ed.* **2001**, *40*, 534–540.
- (3) (a) Popeney, C. S.; Levins, C. M.; Guan, Z. *Organometallics* **2011**, *30*, 2432–2452. (b) Song, D.-P.; Wang, Y.-X.; Mu, H.-L.; Li, B.-X.; Li, Y.-S. *Organometallics* **2011**, *30*, 925–934. (c) Delferro, M.; McInnis, J. P.; Marks, T. J. *Organometallics* **2010**, *29*, 5040–5049. (d) Chen, C.; Luo, S.; Jordan, R. F. *J. Am. Chem. Soc.* **2010**, *132*, 5273–5284. (e) Camacho, D. H.; Guan, Z. *Chem. Commun.* **2010**, *46*, 7879–7893. (f) Berkefeld, A.; Möller, H. M.; Mecking, S. *Organometallics* **2009**, *28*, 4048–4055. (g) Berkefeld, A.; Mecking, S. *J. Am. Chem. Soc.* **2009**, *131*, 1565–1574. (h) Berkefeld, A.; Drexler, M.; Möller, H. M.; Mecking, S. *J. Am. Chem. Soc.* **2009**, *131*, 12613–12622. (i) Noda, S.; Nakamura, A.; Kochi, T.; Chung, L. W.; Morokuma, K.; Nozaki, K. *J. Am. Chem. Soc.* **2009**, *131*, 14088–14100. (j) Chen, C.; Luo, S.; Jordan, R. F. *J. Am. Chem. Soc.* **2008**, *130*, 12892–12893. (k) Wehrmann, P.; Mecking, S. *Organometallics* **2008**, *27*, 1399–1408. (l) Leung, D. H.; Ziller, J. W.; Guan, Z. *J. Am. Chem. Soc.* **2008**, *130*, 7538–7539. (m) Korthals, B.; Goettker-Schnetmann, I.; Mecking, S. *Organometallics* **2007**, *26*, 1311–1316. (n) Popeney, C. S.; Camacho, D. H.; Guan, Z. *J. Am. Chem. Soc.* **2007**, *129*, 10062–10063. (o) Luo, S.; Jordan, R. F. *J. Am. Chem. Soc.* **2006**, *128*, 12072–12073. (p) Wehrmann, P.; Mecking, S. *Macromolecules* **2006**, *39*, 5963–5964. (q) Foley, S. R.; Stockland, R. A.; Shen, H.; Jordan, R. F. *J. Am. Chem. Soc.* **2003**, *125*, 4350–4361. (r) Connor, E. F.; Younkin, T. R.; Henderson, J. I.; Hwang, S.; Grubbs, R. H.; Roberts, W. P.; Litzau, J. *J. Polym. Sci., Part A: Polym. Chem.* **2002**, *40*, 2842–2854.
- (4) (a) Leatherman, M. D.; Brookhart, M. *Macromolecules* **2001**, *34*, 2748–2750. (b) Gates, D. P.; Svejda, S. A.; Onate, E.; Killian, C. M.; Johnson, L. K.; White, P. S.; Brookhart, M. *Macromolecules* **2000**, *33*, 2320–2334. (c) Mecking, S.; Johnson, L. K.; Wang, L.; Brookhart, M. *J. Am. Chem. Soc.* **1998**, *120*, 888–899. (d) Johnson, L. K.; Mecking, S.; Brookhart, M. *J. Am. Chem. Soc.* **1996**, *118*, 267–268. (e) Killian, C. M.; Tempel, D. J.; Johnson, L. K.; Brookhart, M. *J. Am. Chem. Soc.* **1996**, *118*, 11664–11665. (f) Johnson, L. K.; Killian, C. M.; Brookhart, M. *J. Am. Chem. Soc.* **1995**, *117*, 6414–6415.

- (5) (a) Nozaki, K.; Kusumoto, S.; Noda, S.; Kochi, T.; Chung, L. W.; Morokuma, K. *J. Am. Chem. Soc.* **2010**, *132*, 16030–16042. (b) Ito, S.; Munakata, K.; Nakamura, A.; Nozaki, K. *J. Am. Chem. Soc.* **2009**, *131*, 14606–14607. (c) Kochi, T.; Noda, S.; Yoshimura, K.; Nozaki, K. *J. Am. Chem. Soc.* **2007**, *129*, 8948–8949. (d) Kochi, T.; Yoshimura, K.; Nozaki, K. *Dalton Trans.* **2006**, 25–27.
- (6) (a) McCord, E. F.; McLain, S. J.; Nelson, L. T. J.; Ittel, S. D.; Tempel, D.; Killian, C. M.; Johnson, L. K.; Brookhart, M. *Macromolecules* **2007**, *40*, 410–420. (b) Collins, S.; Ziegler, T. *Organometallics* **2007**, *26*, 6612–6623. (c) Zhang, L.; Brookhart, M.; White, P. S. *Organometallics* **2006**, *25*, 1868–1874. (d) Cherian, A. E.; Rose, J. M.; Lobkovsky, E. B.; Coates, G. W. *J. Am. Chem. Soc.* **2005**, *127*, 13770–13771. (e) Liu, W.; Brookhart, M. *Organometallics* **2004**, *23*, 6099–6107. (f) Leatherman, M. D.; Svejda, S. A.; Johnson, L. K.; Brookhart, M. *J. Am. Chem. Soc.* **2003**, *125*, 3068–3081. (g) Gottfried, A. C.; Brookhart, M. *Macromolecules* **2003**, *36*, 3085–3100. (h) Shultz, L. H.; Tempel, D. J.; Brookhart, M. *J. Am. Chem. Soc.* **2001**, *123*, 11539–11555. (i) Shultz, L. H.; Brookhart, M. *Organometallics* **2001**, *20*, 3975–3982. (j) Gottfried, A. C.; Brookhart, M. *Macromolecules* **2001**, *34*, 1140–1142. (k) Tempel, D. J.; Johnson, L. K.; Huff, R. L.; White, P. S.; Brookhart, M. *J. Am. Chem. Soc.* **2000**, *122*, 6686–6700. (l) Svejda, S. A.; Johnson, L. K.; Brookhart, M. *J. Am. Chem. Soc.* **1999**, *121*, 10634–10635. (m) Guan, Z.; Cotts, P. M.; McCord, E. F.; McLain, S. J. *Science* **1999**, *283*, 2059–2062.
- (7) (a) Waltman, A. W.; Younkin, T. R.; Grubbs, R. H. *Organometallics* **2004**, *23*, 5121–5123. (b) Connor, E. F.; Younkin, T. R.; Henderson, J. I.; Waltman, A. W.; Grubbs, R. H. *Chem. Commun.* **2003**, 2272–2273. (c) Younkin, T. R.; Connor, E. F.; Henderson, J. I.; Friedrich, S. K.; Grubbs, R. H.; Bansleben, D. A. *Science* **2000**, *287*, 460–462. (d) Wang, C.; Friedrich, S.; Younkin, T. R.; Li, R. T.; Grubbs, R. H.; Bansleben, D. A.; Day, M. W. *Organometallics* **1998**, *17*, 3149–3151.
- (8) (a) Salata, M. R.; Marks, T. J. *Macromolecules* **2009**, *42*, 1920–1933. (b) Salata, M. R.; Marks, T. J. *J. Am. Chem. Soc.* **2008**, *130*, 12–13. (c) Guo, N.; Stern, C. L.; Marks, T. J. *J. Am. Chem. Soc.* **2008**, *130*, 2246–2261. (d) Amin, S.; Marks, T. J. *J. Am. Chem. Soc.* **2007**, *129*, 2938–2953. (e) Li, H.; Marks, T. J. *Proc. Natl. Acad. Sci. U.S.A.* **2006**, *103*, 15295–15302. (f) Amin, S.; Marks, T. J. *J. Am. Chem. Soc.* **2006**, *128*, 4506–4507. (g) Li, H.; Stern, C. L.; Marks, T. J. *Macromolecules* **2005**, *38*, 9015–9027. (h) Li, H.; Li, L.; Schwartz, D. J.; Metz, M. V.; Marks, T. J.; Liable-Sands, L.; Rheingold, A. L. *J. Am. Chem. Soc.* **2005**, *127*, 14756–14768. (i) Li, H.; Li, L.; Marks, T. J. *Angew. Chem., Int. Ed.* **2004**, *43*, 4937–4940. (j) Guo, N.; Li, L.; Marks, T. J. *J. Am. Chem. Soc.* **2004**, *126*, 6542–6543. (k) Li, H.; Li, L.; Marks, T. J.; Liable-Sands, L.; Rheingold, A. L. *J. Am. Chem. Soc.* **2003**, *125*, 10788–10789.
- (9) (a) Delferro, M.; Marks, T. J. *Chem. Rev.* **2011**, *111*, 2450–2485. (b) Rodriguez, B. A.; Delferro, M.; Marks, T. J. *J. Am. Chem. Soc.* **2009**, *131*, 5902–5919. (c) Rodriguez, B. A.; Delferro, M.; Marks, T. J. *Organometallics* **2008**, *27*, 2166–2168. (d) Weberski Jr., M. P.; Chen, C.; Delferro, M.; Marks, T. J. *Chem. Eur. J.* **2012**, in press.
- (10) Popeney, C. S.; Rheingold, A. L.; Guan, Z. *Organometallics* **2009**, *28*, 4452–4463.
- (11) (a) Bastero, A.; Gottker-Schnetmann, I.; Rohr, C.; Mecking, S. *Adv. Synth. Catal.* **2007**, *349*, 2307–2316. (b) Gottker-Schnetmann, I.; Wehrmann, P.; Röhr, C.; Mecking, S. *Organometallics* **2007**, *26*, 2348–2362. (c) Gottker-Schnetmann, I.; Korthals, B.; Mecking, S. *J. Am. Chem. Soc.* **2006**, *128*, 7708–7709. (d) Wehrmann, P.; Zuideveld, M.; Thomann, R.; Mecking, S. *Macromolecules* **2006**, *39*, 5995–6002. (e) Zuideveld, M. A.; Wehrmann, P.; Röhr, C.; Mecking, S. *Angew. Chem., Int. Ed.* **2004**, *43*, 869–873.
- (12) Soula, R.; Broyer, J. P.; Llauro, M. F.; Tomov, A.; Spitz, R.; Claverie, J.; Drujon, X.; Malinge, J.; Saudemont, T. *Macromolecules* **2001**, *34*, 2438–2442.
- (13) Kuhn, P.; Sémeril, D.; Jeunesse, C.; Matt, D.; Neuburger, M.; Mota, A. *Chem. Eur. J.* **2006**, *12*, 5210–5219.
- (14) Chan, M. S. W.; Deng, L. Q.; Ziegler, T. *Organometallics* **2000**, *19*, 2741–2750.
- (15) (a) So, L.-C.; Liu, C.-C.; Chan, M. C. W.; Lo, J. C. Y.; Sze, K.-H.; Zhu, N. *Chem. Eur. J.* **2012**, *18*, 565–573. (b) Möller, H. M.; Baier, M. C.; Mecking, S.; Talsi, E. P.; Bryliakov, K. P. *Chem. Eur. J.* **2012**, *18*, 848–856.
- (16) (a) Makio, H.; Terao, H.; Iwashita, A.; Fujita, T. *Chem. Rev.* **2011**, *111*, 2363–2449. (b) Mitani, M.; Furuyama, R.; Mohri, J.-I.; Saito, J.; Ishii, S.; Terao, H.; Nakano, T.; Tanaka, H.; Fujita, T. *J. Am. Chem. Soc.* **2003**, *125*, 4293–4305. (c) Ishii, S.-I.; Furuyama, R.; Matsukawa, N.; Saito, J.; Mitani, M.; Tanaka, H.; Fujita, T. *Macromol. Rapid Commun.* **2003**, *24*, 452–456. (d) Mitani, M.; Mohri, J.-I.; Yoshida, Y.; Saito, J.; Ishii, S.; Tsuru, K.; Matsui, S.; Furuyama, R.; Nakano, T.; Tanaka, H.; Kojo, S.-I.; Matsugi, T.; Kashiba, N.; Fujita, T. *J. Am. Chem. Soc.* **2002**, *124*, 3327–3336.
- (17) (a) Chan, M. C. W. *Chem. Asian J.* **2008**, *3*, 18–27. (b) Chan, M. C. W.; Kui, S. C. F.; Cole, J. M.; McIntyre, G. J.; Matsui, S.; Zhu, N.; Tam, K.-H. *Chem. Eur. J.* **2006**, *12*, 2607–2619. (c) Kui, S. C. F.; Zhu, N.; Chan, M. C. W. *Angew. Chem., Int. Ed.* **2003**, *42*, 1628–1632.
- (18) (a) Crespo, M. *Organometallics* **2012**, *31*, 1216–1234. (b) Albrecht, M.; Lindner, M. M. *Dalton Trans.* **2011**, *40*, 8733–8744. (c) Furuya, T.; Kamlet, A. S.; Ritter, T. *Nature* **2011**, *473*, 470–477. (d) Clot, E.; Eisenstein, O.; Jasim, N.; MacGregor, S. A.; McGrady, J. E.; Perutz, R. N. *Acc. Chem. Res.* **2011**, *44*, 333–348. (e) Kuhnel, M. F.; Lentz, D. *Dalton Trans.* **2010**, *39*, 9745–9759. (f) Garcia-Monforte, M. A.; Alonso, P. J.; Fornies, J.; Menjon, B. *Dalton Trans.* **2007**, 3347–3359. (g) de, W. E.; van, K. G.; Deelman, B.-J. *Chem. Soc. Rev.* **1999**, *28*, 37–41. (h) Gordon, A. S. *J. Fluorine Chem.* **1999**, *100*, 227–234.
- (19) (a) Bochmann, M. *Organometallics* **2010**, *29*, 4711–4740. (b) Chen, E. Y. X.; Marks, T. J. *Chem. Rev.* **2000**, *100*, 1391–1434.
- (20) (a) Biffinger, J. C.; Uppaluri, S.; Sun, H.; DiMagno, S. G. *ACS Catal.* **2011**, *1*, 764–771. (b) Wu, L.-L.; Yang, C.-L.; Lo, F.-C.; Chiang, C.-H.; Chang, C.-W.; Ng, K. Y.; Chou, H.-H.; Hung, H.-Y.; Chan, S. I.; Yu, S. S. F. *Chem. Eur. J.* **2011**, *17*, 4774–4787. (c) Bagchi, V.; Bandyopadhyay, D. *Inorg. Chim. Acta* **2010**, *363*, 2786–2790. (d) Hatay, I.; Su, B.; Mendez, M. A.; Corminboeuf, C.; Khoury, T.; Gros, C. P.; Bourdillon, M.; Meyer, M.; Barbe, J.-M.; Ersoz, M.; Zalis, S.; Samec, Z.; Girault, H. H. *J. Am. Chem. Soc.* **2010**, *132*, 13733–13741. (e) Cunningham, M.; McCrate, A.; Nielsen, M.; Swavey, S. *Eur. J. Inorg. Chem.* **2009**, 1521–1525. (f) Li, X.; Tanasova, M.; Vasileiou, C.; Borhan, B. *J. Am. Chem. Soc.* **2008**, *130*, 1885–1893. (g) Rani-Beoram, S.; Meyer, K.; McCrate, A.; Hong, Y.; Nielsen, M.; Swavey, S. *Inorg. Chem.* **2008**, *47*, 11278–11283. (h) Che, C.-M.; Zhang, J.-L.; Zhang, R.; Huang, J.-S.; Lai, T.-S.; Tsui, W.-M.; Zhou, X.-G.; Zhou, Z.-Y.; Zhu, N.; Chang, C. K. *Chem. Eur. J.* **2005**, *11*, 7040–7053. (i) Traylor, T. G.; Byun, Y. S.; Traylor, P. S.; Battioni, P.; Mansuy, D. J. *Am. Chem. Soc.* **1991**, *113*, 7821–7823.
- (21) (a) Hallett, J. P.; Welton, T. *Chem. Rev.* **2011**, *111*, 3508–3576. (b) Yan, N.; Xiao, C.; Kou, Y. *Coord. Chem. Rev.* **2010**, *254*, 1179–1218. (c) Ikegami, S.; Hamamoto, H. *Chem. Rev.* **2009**, *109*, 583–593. (d) Zhang, W. *Green Chem.* **2009**, *11*, 911–920. (e) Tsuda, T.; Hagiwara, R. *J. Fluorine Chem.* **2008**, *129*, 4–13. (f) Liu, S.; Xiao, J. *J. Mol. Catal. A: Chem.* **2007**, *270*, 1–43. (g) Parvulescu, V. I.; Hardacre, C. *Chem. Rev.* **2007**, *107*, 2615–2665. (h) Xue, H.; Verma, R.; Shreeve, J. M. *J. Fluorine Chem.* **2006**, *127*, 159–176. (i) Xue, H.; Shreeve, J. M. *Eur. J. Inorg. Chem.* **2005**, 2573–2580. (j) Adams, D. J.; Cole-Hamilton, D. J.; Hope, E. G.; Pogorzelec, P. J.; Stuart, A. M. *J. Organomet. Chem.* **2004**, *689*, 1413–1417. (k) Bergbreiter, D. E. *Chem. Rev.* **2002**, *102*, 3345–3383. (l) Yoshida, J.; Itami, K. *Chem. Rev.* **2002**, *102*, 3693–3716. (m) Tzschucke, C. C.; Markert, C.; Bannwarth, W.; Roller, S.; Hebel, A.; Haag, R. *Angew. Chem., Int. Ed.* **2002**, *41*, 3964–4000. (n) Kitazume, T. *J. Fluorine Chem.* **2000**, *105*, 265–278.
- (22) (a) Wittmaack, B. K.; Crigger, C.; Guarino, M.; Donald, K. J. *J. Phys. Chem. A* **2011**, *115*, 8743–8753. (b) Dalvi, V. H.; Rossky, P. J. *Proc. Natl. Acad. Sci. U.S.A.* **2010**, *107*, 13603–13607. (c) Rutkowski, K. S.; Herrebout, W. A.; Melikova, S. M.; van, d. V. B. J.; Koll, A. *Chem. Phys.* **2008**, *354*, 71–79. (d) Vijayakumar, S.; Kolandaivel, P. *J. Mol. Struct. (THEOCHEM)* **2006**, *770*, 23–30. (e) Alonso, J. L.; Antolinez, S.; Blanco, S.; Lesarri, A.; Lopez, J. C.; Caminati, W. *J. Am. Chem. Soc.* **2004**, *126*, 3244–3249. (f) Blanco, S.; Lopez, J. C.; Lesarri, A.; Caminati, W.; Alonso, J. L. *ChemPhysChem* **2004**, *5*, 1779–1782.

- (g) Lee, S.; Mallik, A. B.; Fredrickson, D. C. *J. Cryst. Growth Des.* **2004**, *4*, 279–290.  
 (23) (a) Ho, C.-Y.; Chen, Y.-C.; Wong, M.-K.; Yang, D. *J. Org. Chem.* **2005**, *70*, 898–906. (b) Corey, E. J.; Lee, T. W. *Chem. Commun.* **2001**, 1321–1329. (c) Parks, D. J.; Piers, W. E.; Parvez, M.; Atencio, R.; Zaworotko, M. J. *Organometallics* **1998**, *17*, 1369–1377. (d) Corey, E. J.; Rohde, J. J.; Fischer, A.; Azimioara, M. D. *Tetrahedron Lett.* **1997**, *38*, 33–36. (e) Corey, E. J.; Loh, T.-P.; Sarshar, S.; Azimioara, M. *Tetrahedron Lett.* **1992**, *33*, 6945–6948.  
 (24) (a) Qiu, X.-L.; Qing, F.-L. *Eur. J. Inorg. Chem.* **2011**, *2011*, 3261–3278. (b) Panigrahi, K.; Eggen, M.; Maeng, J.-H.; Shen, Q.; Berkowitz, D. B. *Chem. Biol.* **2009**, *16*, 928–936. (c) Berkowitz, D. B.; Karukurichi, K. R.; de la Salud-Bea, R.; Nelson, D. L.; McCune, C. D. *J. Fluorine Chem.* **2008**, *129*, 731–742. (d) O'Hagan, D. *Chem. Soc. Rev.* **2008**, *37*, 308–319. (e) Billard, T.; Langlois, B. R. *Eur. J. Org. Chem.* **2007**, 891–897. (f) Müller, K.; Faeh, C.; Diederich, F. *Science* **2007**, *317* (5846), 1881–1886. (g) Billard, T. *Chem. Eur. J.* **2006**, *12*, 974–979. (h) Hein, M.; Miethchen, R. *Adv. Org. Synth.* **2006**, *2*, 381–429.  
 (i) Kirk, K. L. *J. Fluorine Chem.* **2006**, *127*, 1013–1029. (j) Schlosser, M. *Angew. Chem., Int. Ed.* **2006**, *45*, 5432–5446. (k) Jaeckel, C.; Koksch, B. *Eur. J. Org. Chem.* **2005**, 4483–4503. (l) Leroux, F.; Jeschke, P.; Schlosser, M. *Chem. Rev.* **2005**, *105*, 827–856. (m) Paulini, R.; Mueller, K.; Diederich, F. *Angew. Chem., Int. Ed.* **2005**, *44*, 1788–1805. (n) Biffinger, J. C.; Kim, H. W.; DiMagno, S. G. *ChemBioChem* **2004**, *5*, 622–627. (o) O'Hagan, D.; S. Rzepa, H. *Chem. Commun.* **1997**, 645–652.  
 (25) *Spartan '06*; Wavefunction, Inc., Irvine, CA, 2006.  
 (26) Klein, H. F.; Karsch, H. H. *Chem. Ber.* **1972**, *105*, 2628–2636.  
 (27) Wiencko, H. L.; Kogut, E.; Warren, T. H. *Inorg. Chim. Acta* **2003**, *345*, 199–208.  
 (28) Suenaga, Y.; Umehata, Y.; Hirano, Y.; Minematsu, T.; Pierpont, C. G. *Inorg. Chim. Acta* **2008**, *361*, 2941–2949.  
 (29) Meinhard, D.; Wegner, M.; Kipiani, G.; Hearley, A.; Reuter, P.; Fischer, S.; Marti, O.; Rieger, B. *J. Am. Chem. Soc.* **2007**, *129*, 9182–9191.  
 (30) The monometallic ligand  $(\text{CH}_3)\text{HFI}$  has been structurally characterized. See the Supporting Information.  
 (31) (a) Chen, Q.; Yu, J.; Huang, J. *Organometallics* **2007**, *26*, 617–625. (b) Hu, T.; Tang, L.; Li, X.; Li, Y.; Hu, N. *Organometallics* **2005**, *24*, 2628–2632. (c) Zhang, D.; Jin, G. *Organometallics* **2003**, *22*, 2851–2854. (d) Jenkins, J. C.; Brookhart, M. *Organometallics* **2003**, *22*, 250–256. (e) Liu, W.; Ray, D. G.; Rinaldi, P. L. *Macromolecules* **1999**, *32*, 3817–3819. (f) De Pootter, M.; Smith, P. B.; Dohrer, K. K.; Bennett, K. F.; Meadows, M. D.; Smith, C. G.; Schouwenaars, H. P.; Geerards, R. A. *J. Appl. Polym. Sci.* **1991**, *42*, 399–408.  
 (32) Tamura, K.; Mizukami, H.; Maeda, K.; Watanabe, H.; Uneyama, K. *J. Org. Chem.* **1993**, *58*, 32–35.  
 (33) Boere, R. T.; Klassen, V.; Wolmershauser, G. *Can. J. Chem.* **2000**, *78*, 583–589.  
 (34) Acceptable combustion analyses of  $(\text{CF}_3)\text{FI-Ni-Cl}$  and  $(\text{CH}_3)\text{FI-Ni-Cl}$  were not obtained. Presumably the compounds undergo incomplete combustion.  
 (35) (a) Stewart, J. J. P. *J. Mol. Model.* **2004**, *10*, 155–164. (b) Stewart, J. J. P. *J. Comput. Chem.* **1991**, *12*, 320–341. (c) Stewart, J. J. P. *J. Comput. Chem.* **1989**, *10*, 221–264. (d) Stewart, J. J. P. *J. Comput. Chem.* **1989**, *10*, 209–220.  
 (36) Altomare, A.; Cascarano, G.; Giacovazzo, C.; Guagliardi, A. *J. Appl. Crystallogr.* **1993**, *26*, 343–350.  
 (37) Sheldrick, G. *Acta Crystallogr.* **2008**, *A64*, 112–122.  
 (38) Sheldrick, G. *Cell Now*; Bruker-AXS, Inc., Madison, WI, 2004.  
 (39) Dolomanov, O. V.; Bourhis, L. J.; Gildea, R. J.; Howard, J. A. K.; Puschmann, H. *J. Appl. Crystallogr.* **2009**, *42*, 339.  
 (40) Jenkins, J. C.; Brookhart, M. *J. Am. Chem. Soc.* **2004**, *126*, 5827–5842.  
 (41) For reviews of C–F···H–C interactions, see: (a) D’Oria, E.; Novoa, J. *J. CrystEngComm* **2008**, *10* (4), 423–436. (b) Reichenbacher, K.; Suss, H. I.; Hulliger, J. *Chem. Soc. Rev.* **2005**, *34*, 22–30. (c) Hyla-Kryspin, I.; Haufe, G.; Grimme, S. *Chem. Eur. J.* **2004**, *10*, 3411–3422. (d) Desiraju, G. R. *Acc. Chem. Res.* **2002**, *35*, 565–573. (e) Parsch, J.; Engels, J. W. *J. Am. Chem. Soc.* **2002**, *124*, 5664–5672. (f) Shimoni, L.; Carrell, H. L.; Glusker, J. P.; Coombs, M. M. *J. Am. Chem. Soc.* **1994**, *116*, 8162–8168.  
 (42) See the Supporting Information.  
 (43) Thomas, I. R.; Bruno, I. J.; Cole, J. C.; Macrae, C. F.; Pidcock, E.; Wood, P. A. *J. Appl. Crystallogr.* **2010**, *43*, 362–366.  
 (44) (a) Haynes, W. M. *CRC Handbook of Chemistry and Physics*, 91st ed.; CRC Press: Boca Raton, FL, 2010–2011. (b) Rowland, R. S.; Taylor, R. *J. Phys. Chem.* **1996**, *100*, 7384–7391. (c) Bondi, A. *J. Phys. Chem.* **1964**, *68*, 441–451.  
 (45) (a) Riccieri, P.; Zinato, E.; Aliboni, A. *Inorg. Chem.* **1997**, *36*, 2279–2286. (b) Glerup, J.; Moensted, O.; Schaeffer, C. E. *Inorg. Chem.* **1976**, *15*, 1399–1407. (c) Flint, C. D.; Matthews, A. P. *Inorg. Chem.* **1975**, *14*, 1008–1014.  
 (46) The ethyl group at 70% occupancy displays a relatively close solid state  $(\text{C})\text{F}\cdots\text{H}_\beta(\text{C})$  contact of 3.66 Å, whereas the minor ethyl conformation (30%) displays a longer  $(\text{C})\text{F}\cdots\text{H}_\beta(\text{C})$  distance of 3.81 Å.  
 (47) (a) Henrici-Olivé, G.; Olivé, S. *Fortschritte der Hochpolymeren-Forschung*; Springer: Berlin, Heidelberg, Germany: 1974; Vol. 15, pp 1–30. (b) Flory, P. J. *J. Am. Chem. Soc.* **1940**, *62*, 1561–1565. (c) Schulz, G. V. *Z. Phys. Chem., B* **1935**, *30*, 379–398. (d) Schulz, G. V. *Z. Phys. Chem., B* **1939**, *43*, 25–46.  
 (48) Talarico, G.; Budzelaar, P. H. M. *Organometallics* **2008**, *27*, 4098–4107.  
 (49) For DFT calculations on ethylene polymerization mediated by neutral Ni(II) catalysts, see: (a) Deng, L.; Margl, P.; Ziegler, T. *J. Am. Chem. Soc.* **1997**, *119*, 1094–1100. (b) Deng, L.; Woo, T. K.; Cavallo, L.; Margl, P. M.; Ziegler, T. *J. Am. Chem. Soc.* **1997**, *119*, 6177–6186.  
 (50) Ethylene polymerizations mediated by anilinotropenate Ni(II) catalysts also display a proportional  $M_w$  increase and branching decrease with increasing ethylene pressure; β-H elimination was reported to be the predominant chain-transfer pathway. See: Hicks, F. A.; Jenkins, J. C.; Brookhart, M. *Organometallics* **2003**, *22*, 3533–3545.  
 (51) Berkefeld, A.; Mecking, S. *J. Am. Chem. Soc.* **2009**, *131* (4), 1565–1574.  
 (52)  $(\text{C}=\text{N}_{\text{CF}_3})\text{FI-Ni}$  exhibits a dramatic decrease in ethylene polymerization activity at elevated temperatures (60 °C). This decrease in activity is accompanied by the formation of Ni(0), which is indicative of catalyst deactivation.  
 (53) For general discussions of the conformational aspects of β-H elimination mechanisms, see: (a) Hartwig, J. In *Organotransition Metal Chemistry: From Bonding to Catalysis*; University Science Books: Sausalito, CA, 2010; pp 398–410. (b) Crabtree, R. H. *The Organometallic Chemistry of the Transition Metals*, 4th ed.; Wiley: Hoboken, NJ, 2005.  
 (54) (a) Zuccaccia, D.; Bellachoma, G.; Cardaci, G.; Ciancaleoni, G.; Zuccaccia, C.; Clot, E.; Macchioni, A. *Organometallics* **2007**, *26*, 3930–3946. (b) Zuccaccia, C.; Stahl, N. G.; Macchioni, A.; Chen, M.-C.; Roberts, J. A.; Marks, T. J. *J. Am. Chem. Soc.* **2004**, *126*, 1448–1464. (c) Macchioni, A. *Eur. J. Inorg. Chem.* **2003**, *2003*, 195–205. (d) Yu, C.; Levy, G. C. *J. Am. Chem. Soc.* **1984**, *106*, 6533–6537.  
 (55) Belt, S. T.; Helliwell, M.; Jones, W. D.; Partridge, M. G.; Perutz, R. N. *J. Am. Chem. Soc.* **1993**, *115*, 1429–1440.  
 (56) Bell, T. W.; Helliwell, M.; Partridge, M. G.; Perutz, R. N. *Organometallics* **1992**, *11*, 1911–1918.  
 (57) Fekl, U.; van Eldik, R.; Lovell, S.; Goldberg, K. I. *Organometallics* **2000**, *19*, 3535–3542.  
 (58) (a) Abraham, R.; Mobli, M., *Modeling <sup>1</sup>H NMR Spectra of Organic Compounds: Theory, Applications, and NMR Prediction Software*; Wiley: Chichester, U.K., 2008; (b) Abraham, R. J.; Mobli, M.; Smith, R. J. *Magn. Reson. Chem.* **2003**, *41*, 26–36. (c) Mallory, F. B.; Mallory, C. W.; Butler, K. E.; Lewis, M. B.; Xia, A. Q.; Luzik, E. D.; Fredenburgh, L. E.; Ramanjulu, M. M.; Van, Q. N.; Franch, M. M.; Freed, D. A.; Wray, C. C.; Hann, C.; Nerz-Stormes, M.; Carroll, P. J.; Chirlan, L. E. *J. Am. Chem. Soc.* **2000**, *122*, 4108–4116. (d) Abraham, R. J.; Warne, M. A.; Griffiths, L. J. *Chem. Soc., Perkin Trans. 2* **1997**, 203–208. (e) Abraham, R. J.; Edgar, M.; Griffiths, L.; Powell, R. L. J. *Chem. Soc., Perkin Trans. 2* **1995**, 561–567.

- (59) Macchioni, A.; Magistrato, A.; Orabona, I.; Ruffo, F.; Rothlisberger, U.; Zuccaccia, C. *New J. Chem.* **2003**, *27*, 455–458.
- (60) Macura, S.; Ernst, R. R. *Mol. Phys.* **1980**, *41*, 95.
- (61) (a) Mountford, A. J.; Lancaster, S. J.; Coles, S. J.; Horton, P. N.; Hughes, D. L.; Hursthouse, M. B.; Light, M. E. *Organometallics* **2006**, *25*, 3837–3847. (b) Caminati, W.; López, J. C.; Alonso, J. L.; Grabow, J.-U. *Angew. Chem., Int. Ed.* **2005**, *44*, 3840–3844. (c) Howard, J. A. K.; Hoy, V. J.; O'Hagan, D.; Smith, G. T. *Tetrahedron* **1996**, *52*, 12613–12622. (d) Shimoni, L.; Glusker, J. *Struct. Chem.* **1994**, *5*, 383–397.
- (62) Thalladi, V. R.; Weiss, H.-C.; Bläser, D.; Boese, R.; Nangia, A.; Desiraju, G. R. *J. Am. Chem. Soc.* **1998**, *120*, 8702–8710.